Computazione quantistica con sistemi ottici e a microonde

A brief introduction to quantum computation with infinite-dimensional systems

Alessandro Ferraro

University of Milan

Outline

Why and how do we use infinite-dimensional systems?

What do we gain?

What is a genuine resource for quantum computational advantage?

Discrete variables

(finite dimension, qubits)

$|1\rangle$

$|0\rangle$

Spin

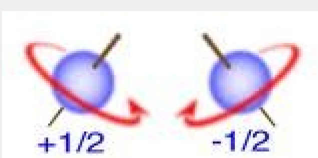

Optics
(polarization)

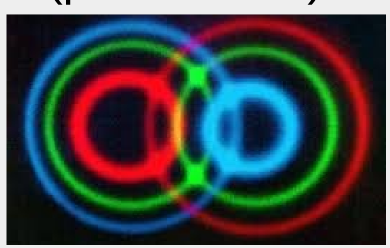

Circuit-QED
(transmon)

Many quantum systems are “CVs”

Discrete variables

(finite dimension, qubits)

$|1\rangle$ ————————

$|0\rangle$ ————————

Continuous variables (CVs)

(infinite dimension, distinguishable bosons)

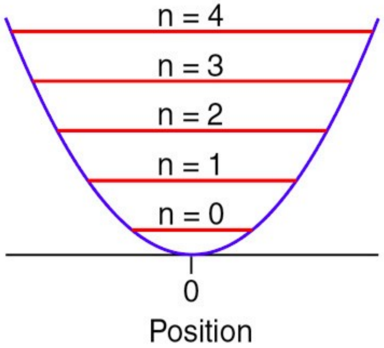

$\hat{q}\ ,\hat{p}$

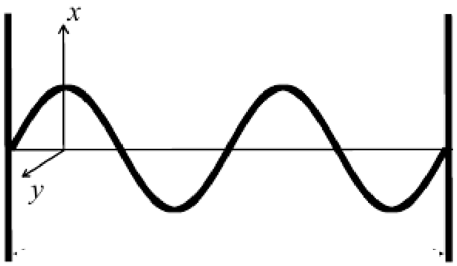

$$\hat{H} = \frac{1}{2}(\hat{p}^2 + \omega^2 \hat{q}^2)$$

Spin

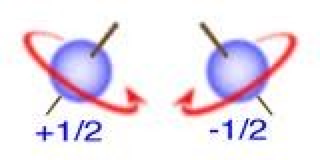

Optics
(polarization)

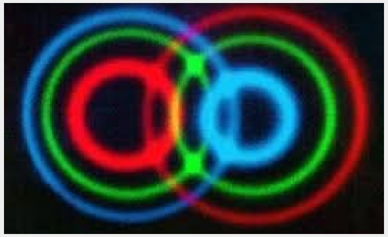

Circuit-QED
(transmon)

Mechanical
oscillators

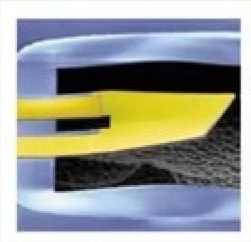

Optics
(quadratures)

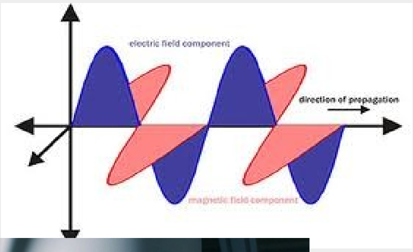

Circuit-QED
(microwave)

Can we use continuous variables to process quantum information?

(Classical Information) History says: **"yes..."**

Differential analyzer, 1938
(University of Cambridge)

"... but you'd better digitize it"

Digitizing classical CVs:
encoding classical bits in classical continuous variables

Physical

Logical

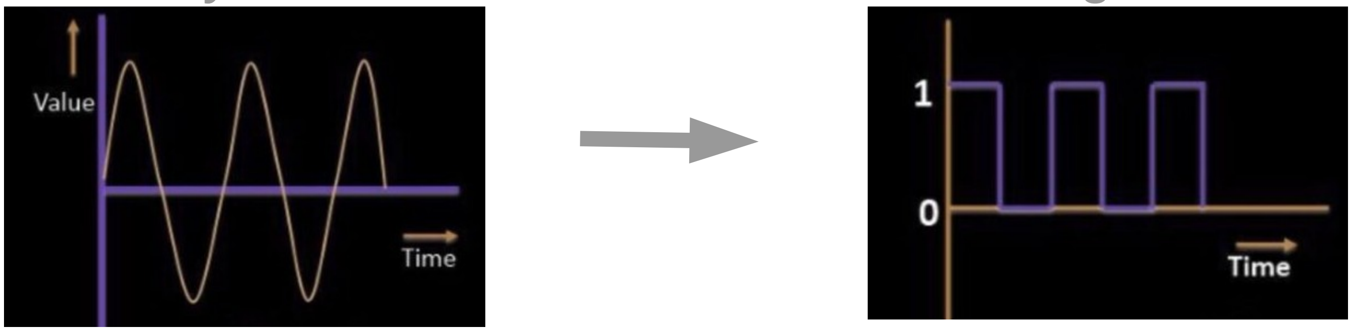

Digitizing classical CVs:
encoding classical bits in classical continuous variables

Physical

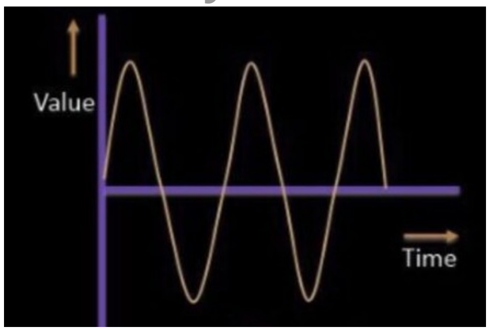

Logical

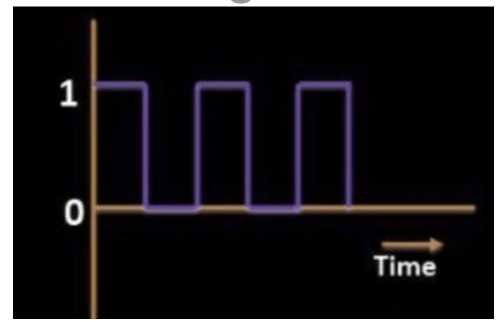

Digitizing quantum CVs (bosonic codes):
encoding qubits in quantum continuous variables

Physical

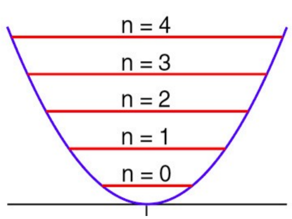

Logical

Identify a two-dimensional Hilbert space within the infinite-dimensional Hilbert space of the physical system

$$\{|0\rangle, |1\rangle, |2\rangle, \ldots\} \rightarrow \{|0\rangle_L, |1\rangle_L\}$$

Bosonic code (I): Fock encoding

Encoded qubits (wavefunction)	Pros	Cons
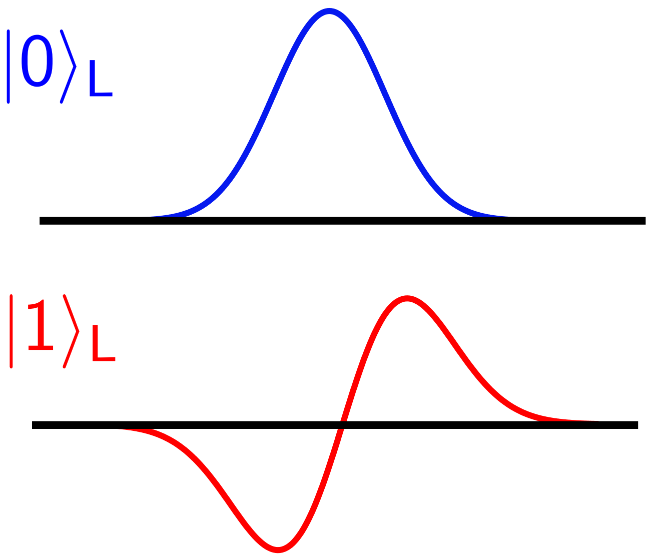	Natural choice Experimentally "easy" to generate Benchmark	Not resilient to noise (e.g., losses)

Outline

Why and how do we use infinite-dimensional systems?

Most quantum systems are infinite-dimensional
but we have to digitize them (bosonic codes)

What do we gain?

What is a genuine resource for quantum computational advantage?

Coherent states

$|0\rangle$

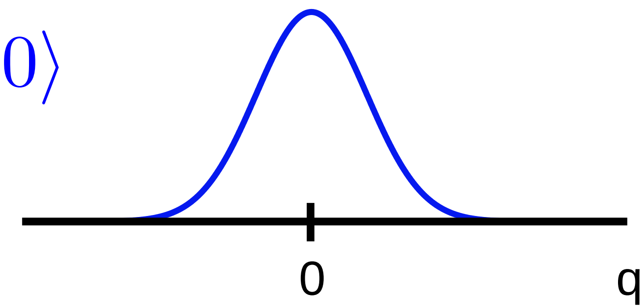

$$\psi(q) \propto e^{-\frac{1}{2}q^2}$$

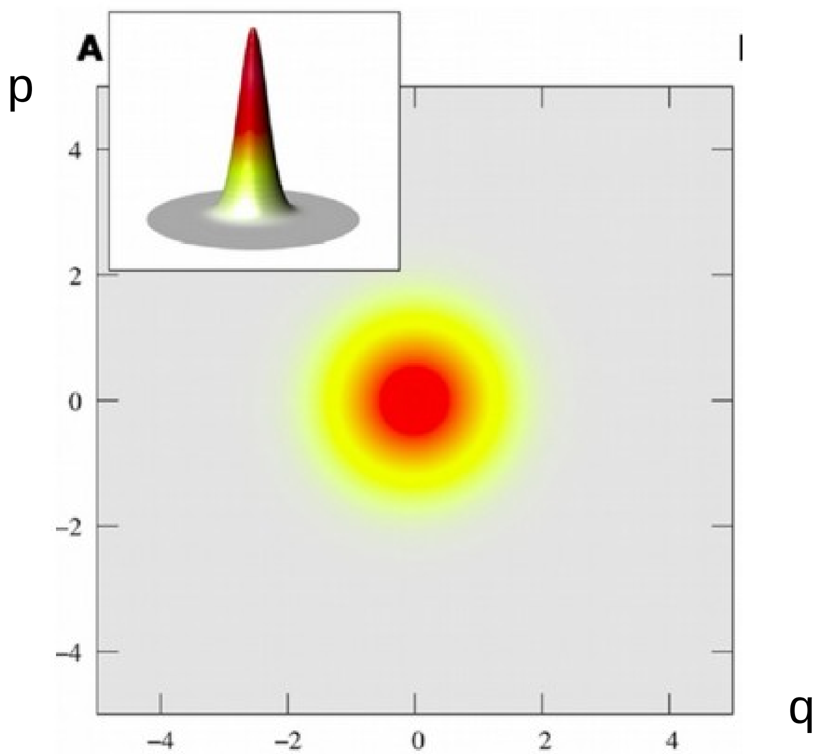

$|\alpha\rangle$

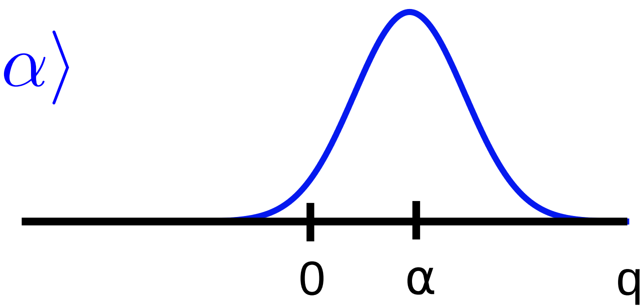

$$\psi(q) \propto e^{-\frac{1}{2}(q-\alpha)^2}$$

$$|\alpha\rangle = e^{-\frac{|\alpha|^2}{2}} \sum_{n=0}^{\infty} \frac{\alpha^n}{\sqrt{n!}} |n\rangle$$

Bosonic codes (II): the cat code

$$|\mathrm{cat}_+\rangle \propto |\alpha\rangle + |-\alpha\rangle$$

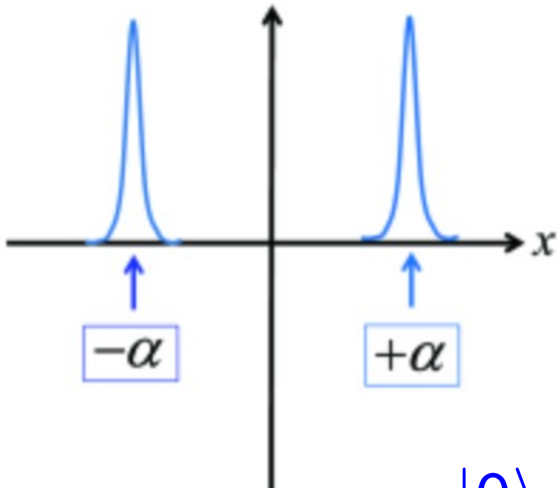

$|0\rangle_L$

$$|\mathrm{cat}_-\rangle \propto |\alpha\rangle - |-\alpha\rangle$$

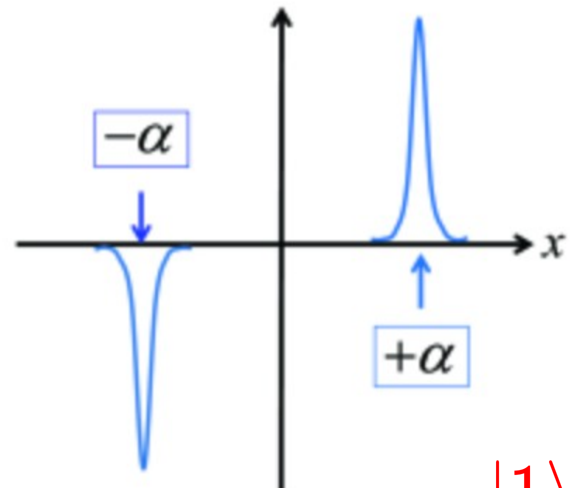

$|1\rangle_L$

Two locations
(dead/alive)
at once

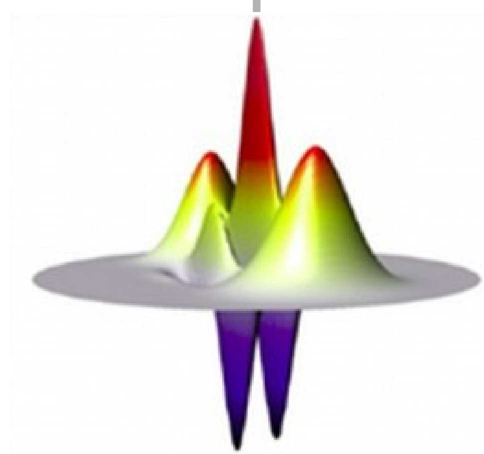

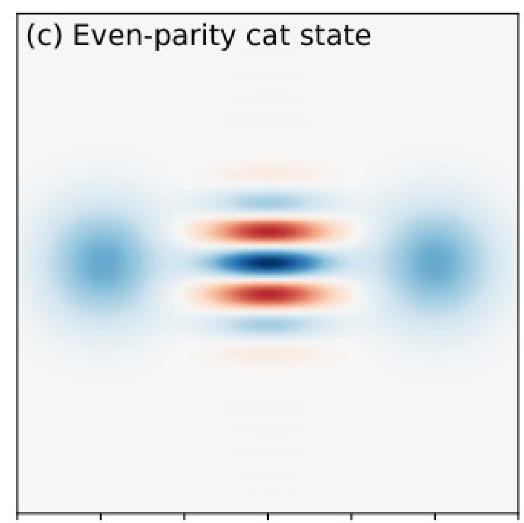

Note: - if one photon is lost, not all information is lost
- the Wigner function displays negative values

Bosonic codes (III): binomial codes

$$|0\rangle_{\mathsf{L}} = \frac{1}{2}|0\rangle + \frac{\sqrt{3}}{2}|4\rangle \quad \xrightarrow{\text{single-excitation loss}} \quad |3\rangle$$

$$|1\rangle_{\mathsf{L}} = |2\rangle \quad \longrightarrow \quad |1\rangle$$

Even (Fock) parity

Odd parity

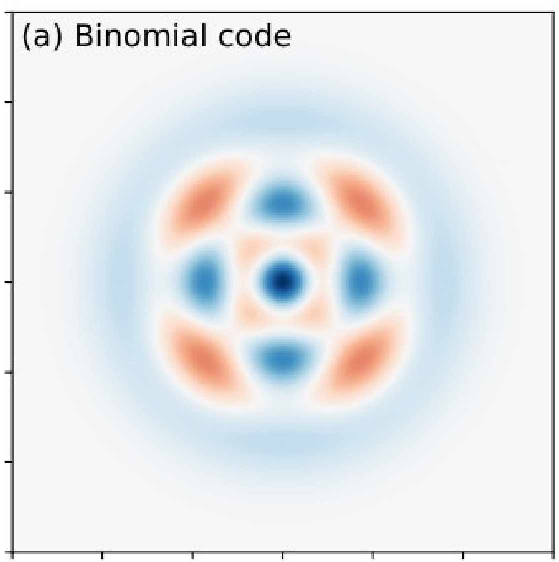

Resilient to single-excitation loss:

- The states are left orthogonal
- Error identification without gaining information on the logical qubit

  (parity measurements)
- Error correction (ancillary systems)

Note: the Wigner function displays negative values

Discrete variables

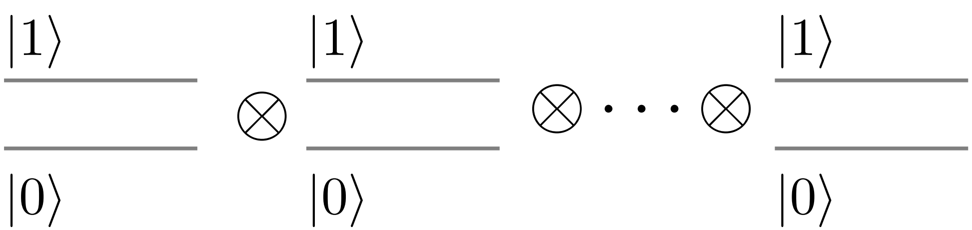

3-qubit repetition code

$$|0\rangle \rightarrow |0_L\rangle \equiv |000\rangle$$
$$|1\rangle \rightarrow |1_L\rangle \equiv |111\rangle$$

To protect 1 logical qubit from arbitrary single qubit errors at least 5 physical qubits are needed

(Steane code)

Hardware efficiency:
bosonic codes do not need additional physical systems

Discrete variables

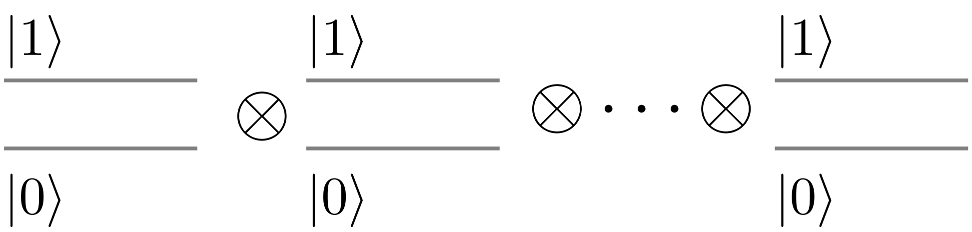

3-qubit repetition code

$$|0\rangle \rightarrow |0_L\rangle \equiv |000\rangle$$
$$|1\rangle \rightarrow |1_L\rangle \equiv |111\rangle$$

To protect 1 logical qubit from arbitrary single qubit errors at least 5 physical qubits are needed

(Steane code)

Continuous variables

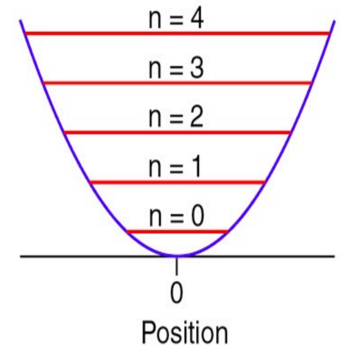

$$|\mathrm{cat}_+\rangle \propto |\alpha\rangle + |-\alpha\rangle$$
$$|\mathrm{cat}_-\rangle \propto |\alpha\rangle - |-\alpha\rangle$$

Cat code

$$|0\rangle_\mathrm{L} = \frac{1}{2}|0\rangle + \frac{\sqrt{3}}{2}|4\rangle$$
$$|1\rangle_L = |2\rangle$$

Binomial code

Extending the lifetime of a quantum bit with error correction in superconducting circuits

Nature **536**, 441–445 (2016) Ofek, N., Petrenko, A., Heeres, R. *et al.*

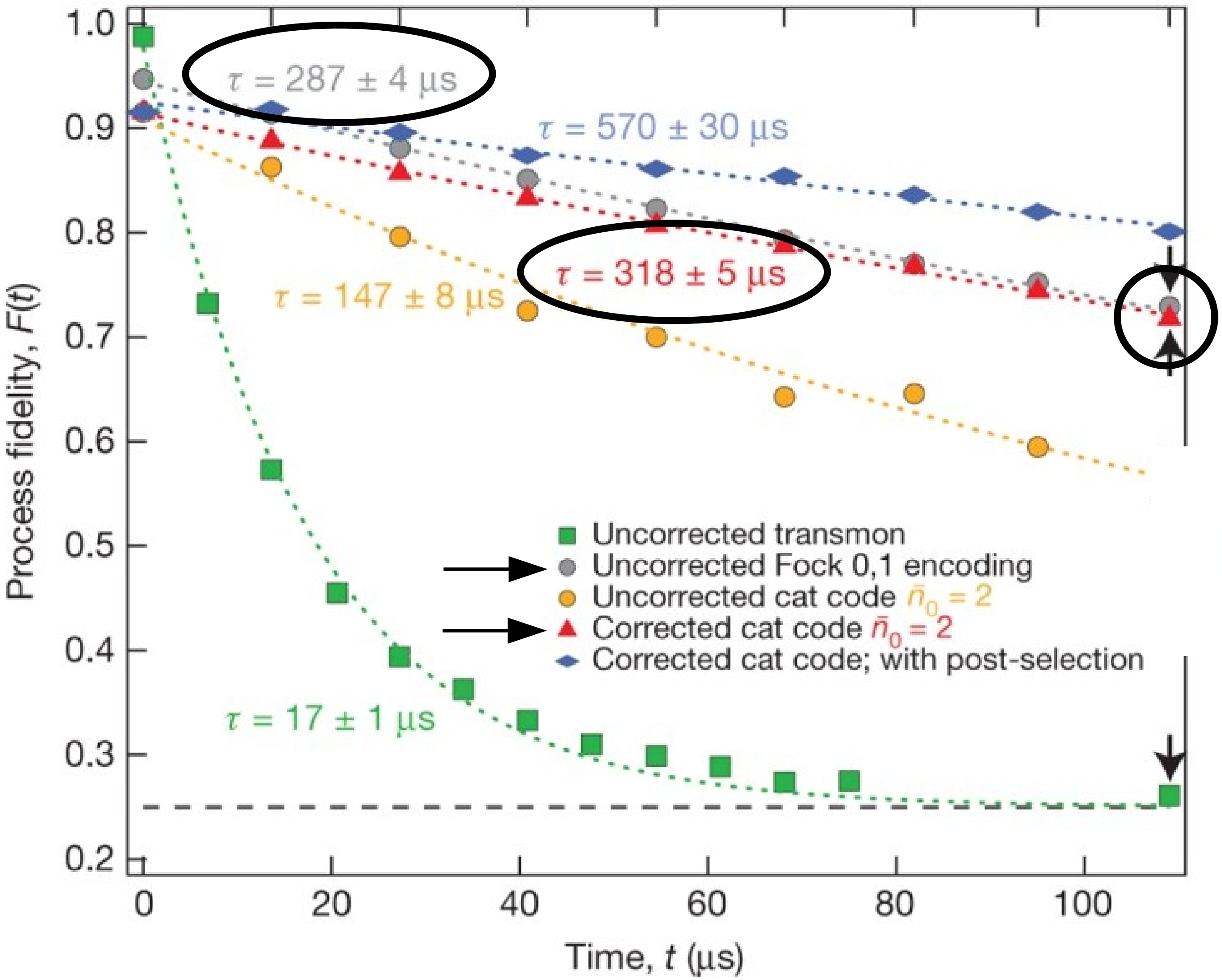

$$F(t) = \frac{1}{4}(1 + 3Ae^{-t/\tau})$$

Break-even: life-time ratio approx 1.1

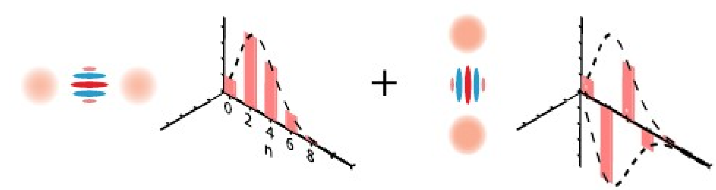

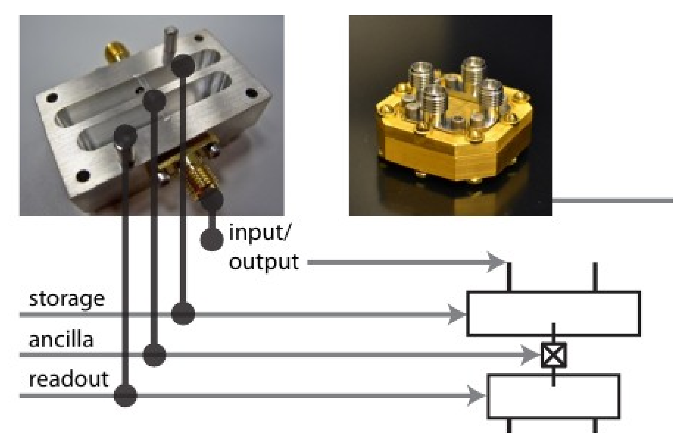

Bosonic codes (IV): GKP codes

PHYSICAL REVIEW A, VOLUME 64, 012310

Encoding a qubit in an oscillator

Daniel Gottesman,[1,2,*] Alexei Kitaev,[1,†] and John Preskill[3,‡]

(Received 9 August 2000; published 11 June 2001)

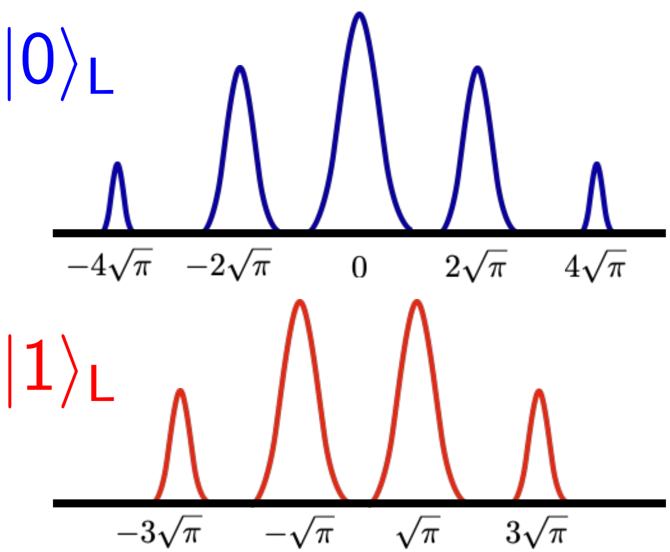

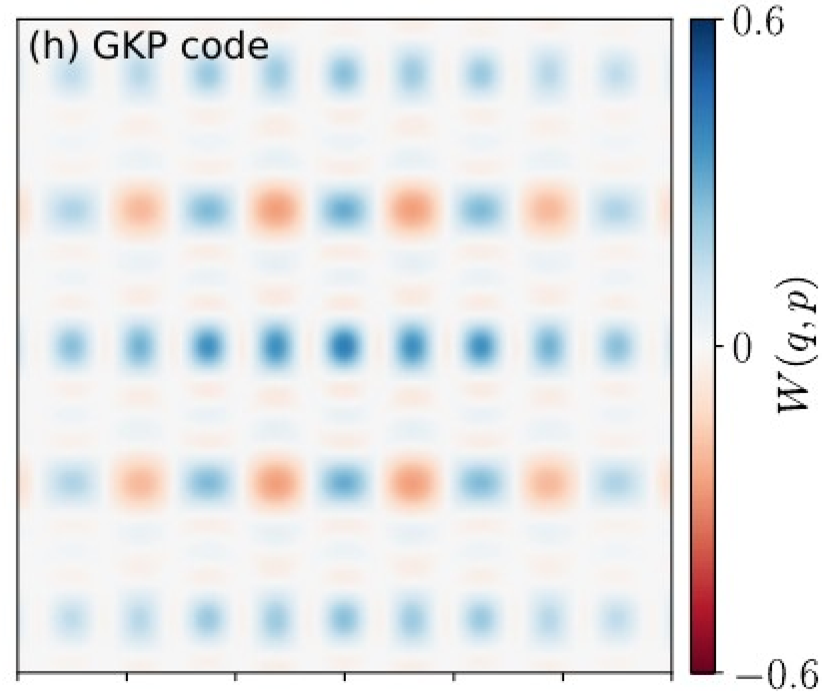

Note: As long as the overlap is small, errors can be corrected for.
The Wigner function displays negative values

Encoding a qubit in a trapped-ion mechanical oscillator

C. Flühmann, T. L. Nguyen, M. Marinelli, V. Negnevitsky, K. Mehta & J. P. Home

Nature **566**, 513–517 (2019) | Cite this article

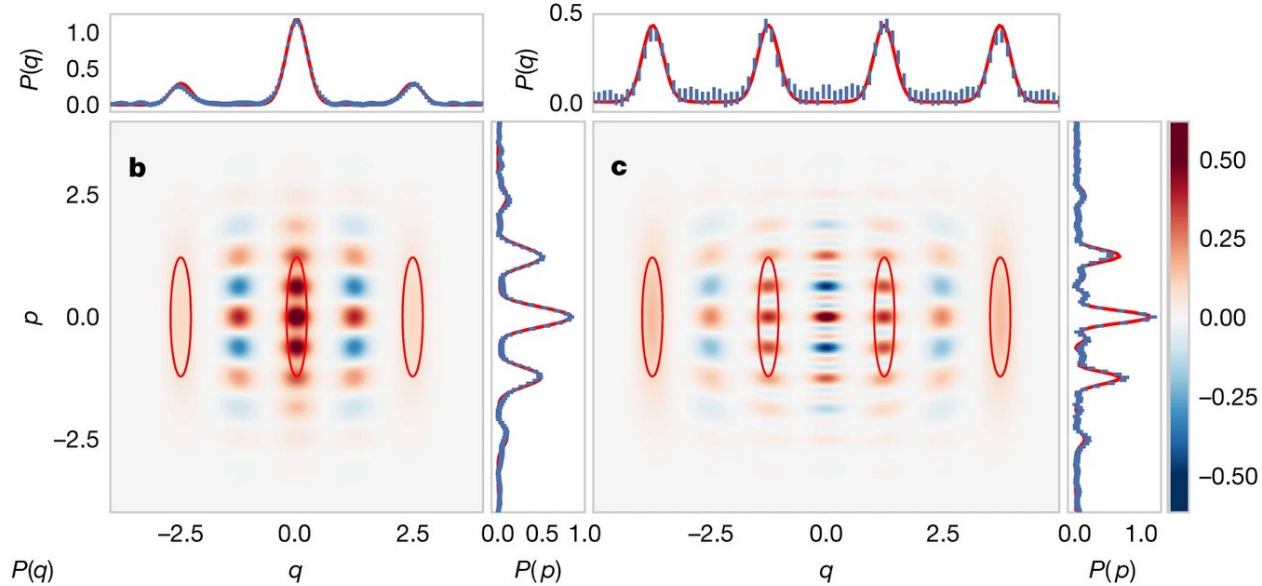

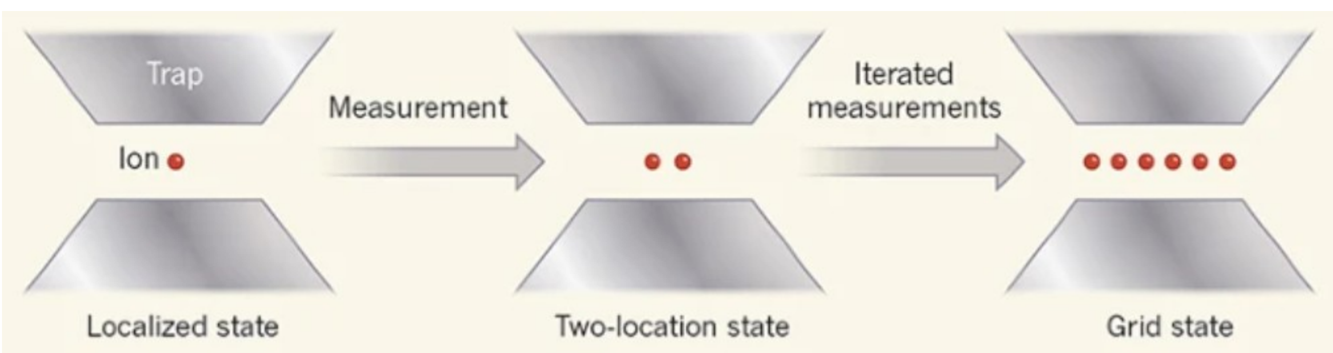

Associated Content

Promising ways to encode and manipulate quantum information

Alessandro Ferraro

Nature | **News & Views** | 27 Feb 2019

Additional advantage of CV systems: record-large number of entangled & controllable systems

Invited Article: Generation of one-million-mode continuous-variable cluster state by unlimited time-domain multiplexing

APL Photonics 1, 060801 (2016); https://doi.org/10.1063/1.4962732

Jun-ichi Yoshikawa[1], Shota Yokoyama[1,2], Toshiyuki Kaji[1], Chanond Sornphiphatphong[1], Yu Shiozawa[1], Kenzo Makino[1], *and* Akira Furusawa[1,a)]

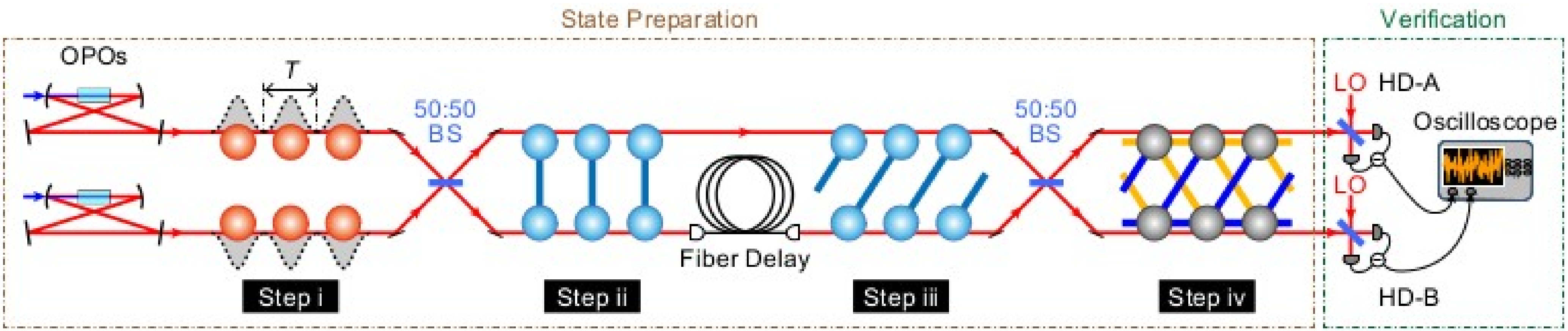

Quantum computational advantage with a programmable photonic processor

Nature **606**, 75–81 (2022) Madsen, L.S., Laudenbach, F., Askarani, M.F. *et al.*

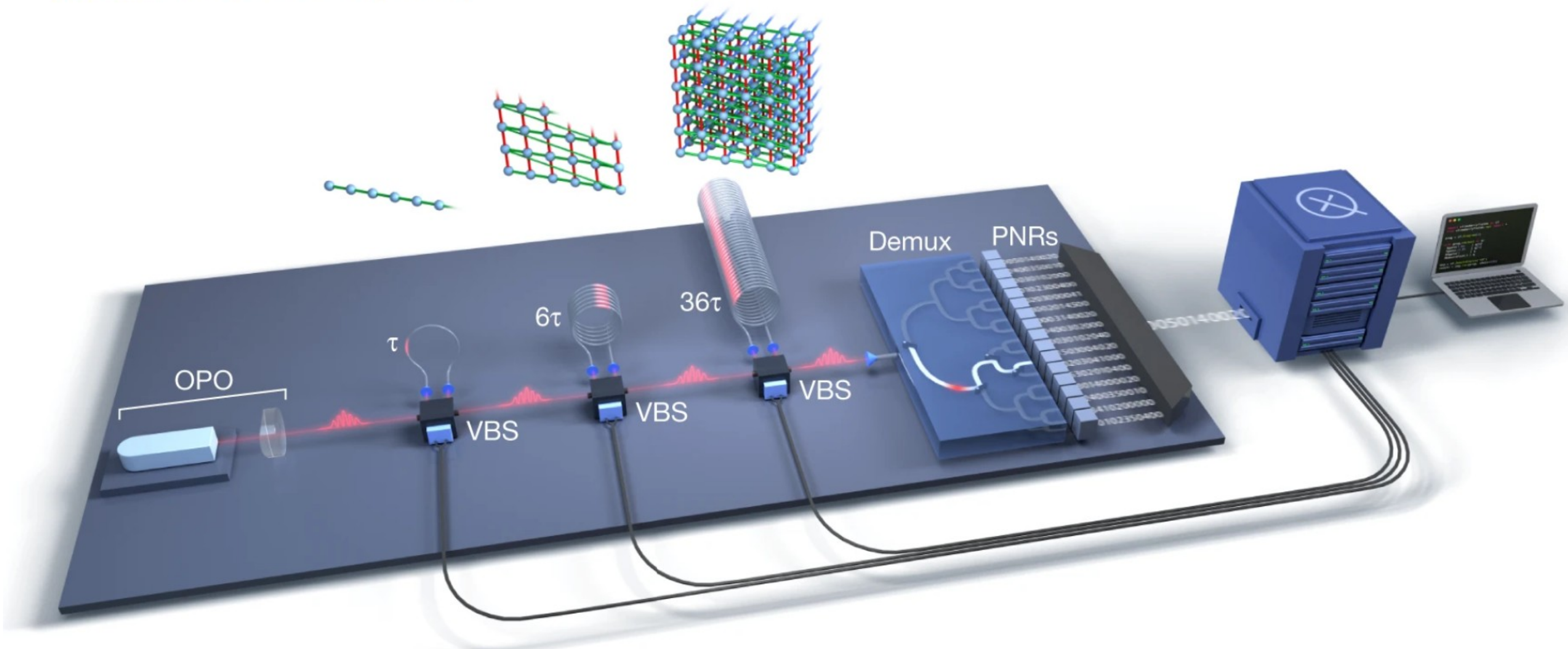

Deterministic generation of an entangled state of <u>216 modes</u>, with mean photon number 125, and <u>1,296 programmable real parameters</u>.

Sampling (approx 10^{12} times) **faster** than a classical computer.

Outline

Why and how do we use infinite-dimensional systems?

Most quantum systems are infinite-dimensional
but we have to digitize them (bosonic codes)

What do we gain?

Excellent performances for noise-resilience and scalability

What is a genuine resource for quantum computational advantage?

Bosonic circuits

A generic bosonic circuits is composed of:

- Initial states $|\psi\rangle$
- Gates
- Measurements

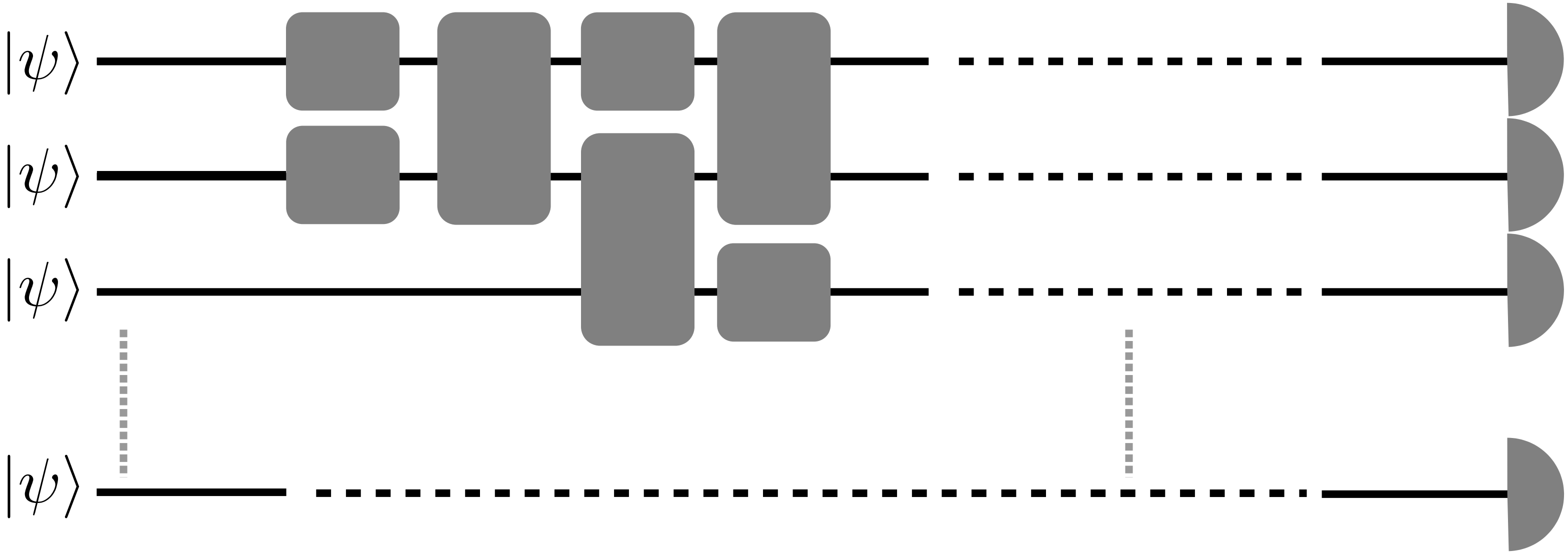

Which type of components are needed for quantum computational advantage?

Some bosonic circuits provide no quantum advantage

Gaussian circuits with vacuum input can be simulated efficiently on a classical computer:

- CV circuits initialized in $|\mathrm{vac}\rangle$
- Gaussian gates  (linear and quadratic interactions)
- Position (homodyne) measurements  and conditioned Gaussian gates

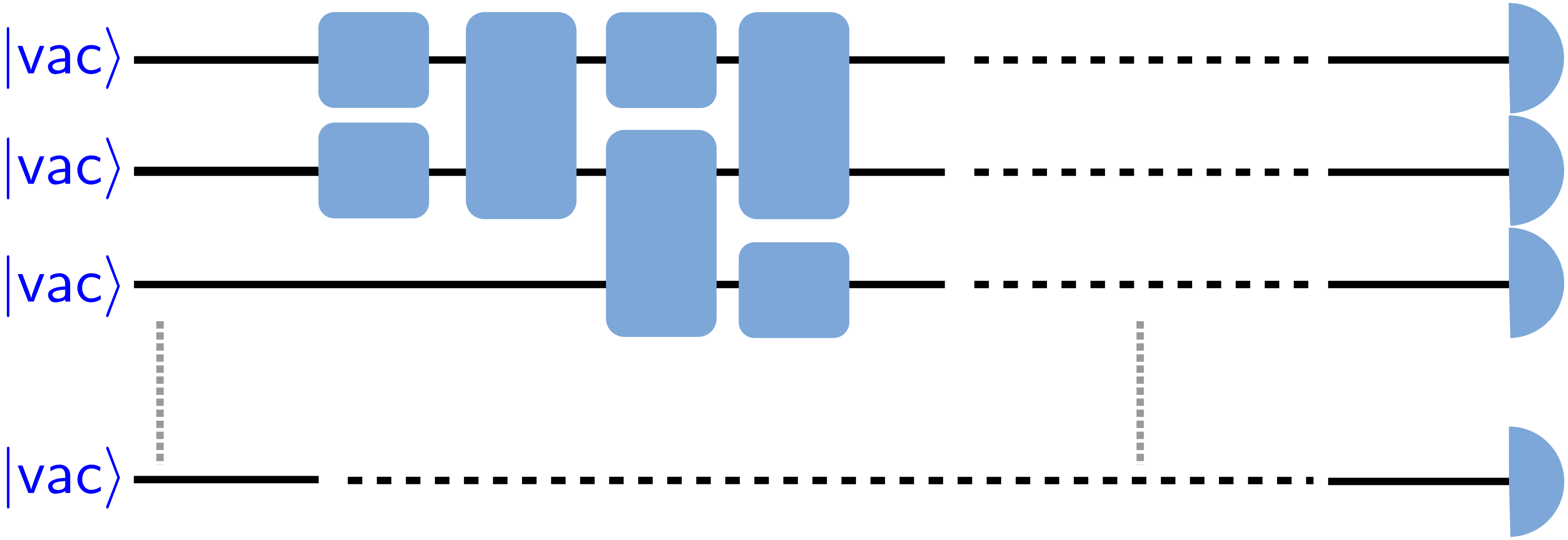

[Bartlett et al., PRL 2002]

Wigner negativity is necessary for quantum advantage

[Mari et al. PRL 2012; Veitch et al NJP 2013; Rahimi-Keshari et al.,PRX 2016]

GKP states provide quantum advantage

Adding GKP inputs make these circuit universal (quantum advantage):

- CV systems initialized in $|0\rangle_{GKP}$ and vacuum states $|vac\rangle$
- Gaussian gates (linear and quadratic interactions)
- Homodyne measurements and Gaussian gates conditioned on outcomes

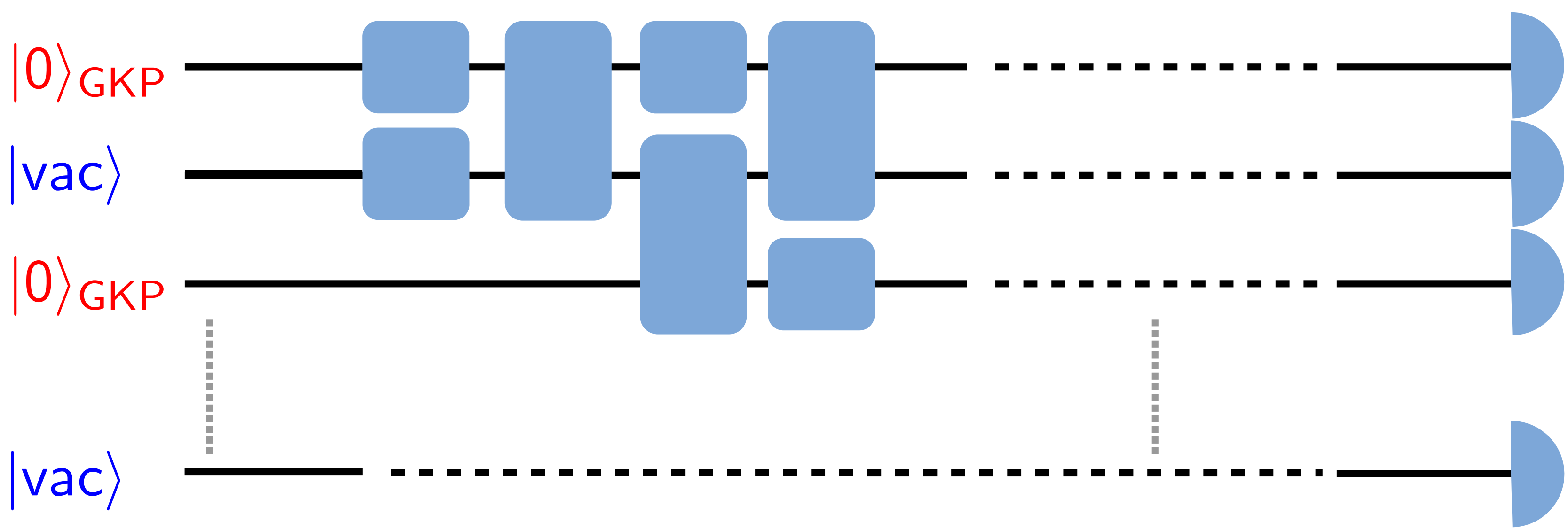

[Baragiola et al., PRL ‘19]

Resource theory of CV quantum computation (Wigner negativity)

State space

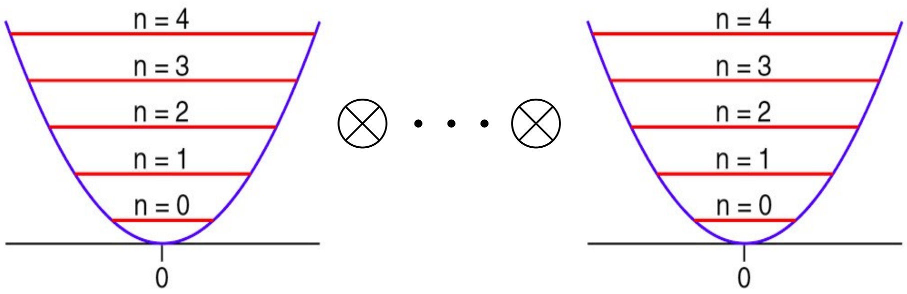

Free states

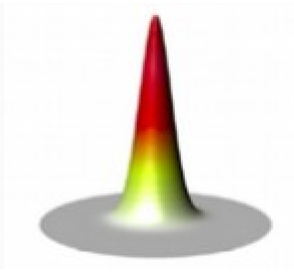

Free operations

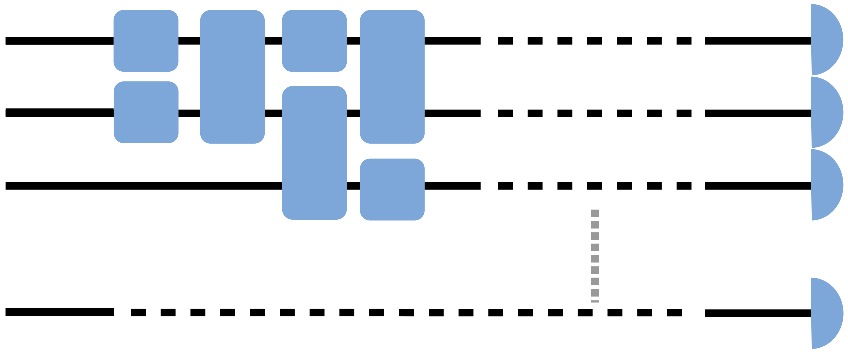

Resources

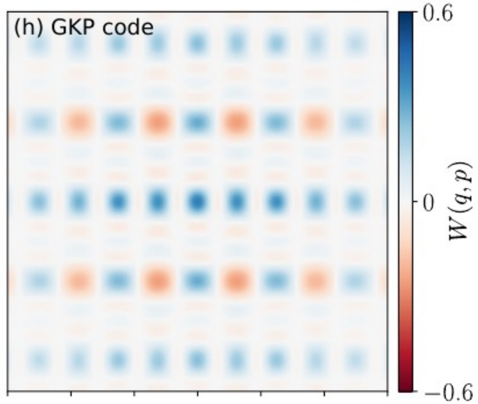

[Albarelli, Genoni, Paris, AF, PRA 2018]

A resource quantifier: Wigner Logarithmic Negativity

The negative volume of the Wigner function is a natural candidate.

Define the Wigner Logarithmic Negativity as:

$$\mathsf{M}(\rho) = \log\left(\int \mathrm{d}\mathbf{r}\ |\mathsf{W}_\rho(\mathbf{r})|\right)$$

It is an additive & computable monotone!

[Albarelli, Genoni, Paris, AF, PRA 2018]

Comparison of resources

Fock states are not the most resourceful states at fixed energy

[McConnell, AF, Puebla, arXiv:2209.07958]

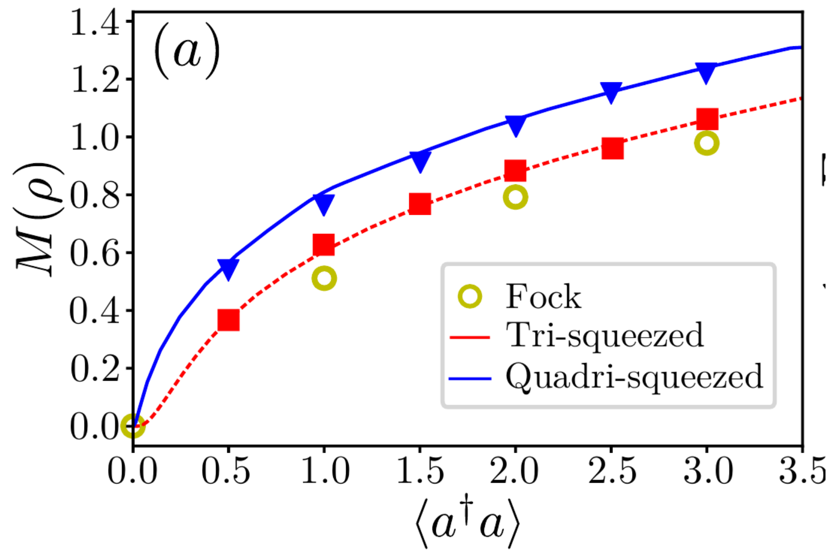

Conversion between resources

Probabilistic conversion of three-squeezed states to cubic-phase states with high fidelity (F=99.6, prob 7%)

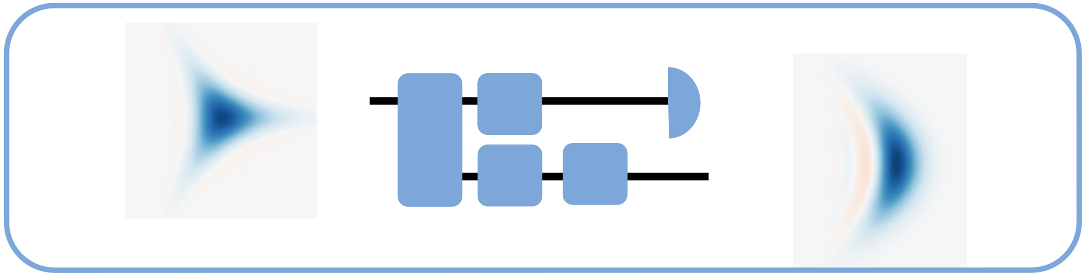

[Zheng, …, AF, Ferrini, PRX Quantum 2021; Hahn,,Holmvall, Stadler, Ferrini, AF, PRA 2022]

Quantification of DVs resources: GKP-magic

$$|\psi\rangle = \sum\nolimits_{i\in\mathbb{F}_2^n} c_i\,|i\rangle$$

$$|i\rangle = |i_1 i_2 \dots i_n\rangle \quad i_l \in \{0,1\}$$

$$\mathcal{G}(|\psi\rangle) \equiv \log_2\left(\sum_{i,j\in\mathbb{F}_2^n}\left|\sum_{k\in\mathbb{F}_2^n}\frac{(-1)^{i\cdot k}}{2^n}c_k\,c_{k+j}^*\right|\right)$$

[Hahn, AF, Ferrini, Garcia-Alvarez, PRL 2022]

Some bosonic circuits provide no quantum advantage

Gaussian circuits with vacuum input can be simulated efficiently on a classical computer:

- CV circuits initialized in $|\text{vac}\rangle$
- Gaussian gates  (linear and quadratic interactions)
- Position (homodyne) measurements  and conditioned Gaussian gates

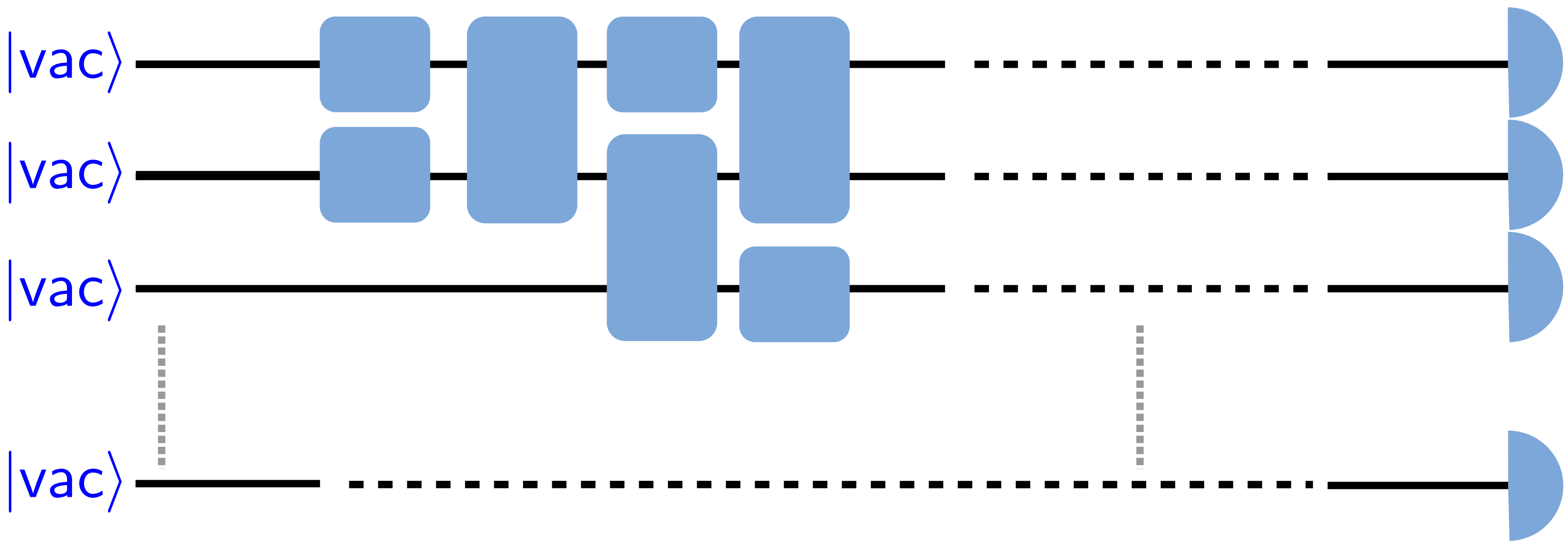

[Bartlett et al., PRL 2002]

Wigner negativity is ncessary for quantum advantage

[Mari et al. PRL 2012; Veitch et al NJP 2013; Rahimi-Keshari et al.,PRX 2016]

And if we consider GKP input?

Gaussian circuits with **<u>only</u>** 0-GKP input can be simulated efficiently on a classical computer:

- CV circuits initialized in $|0\rangle_{\text{GKP}}$
- Gaussian gates  (linear and quadratic interactions, …)
- Position (homodyne) measurements 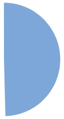 and conditioned Gaussian gates

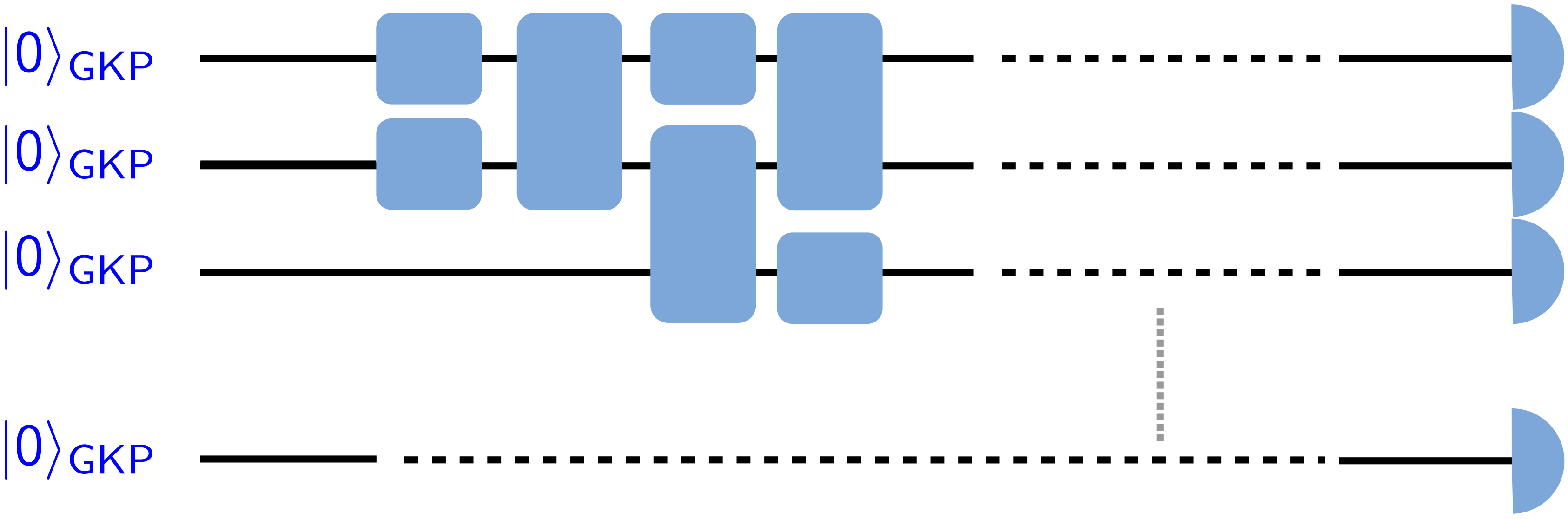

No quantum advantage despite Wigner negativity

[García-Álvarez, Calcluth, AF, Ferrini, PRR 2020; Calcluth, AF, Ferrini, Quantum 2022 & arXiv:2205.09781]

GKP states provide quantum advantage to otherwise simulatable circuits

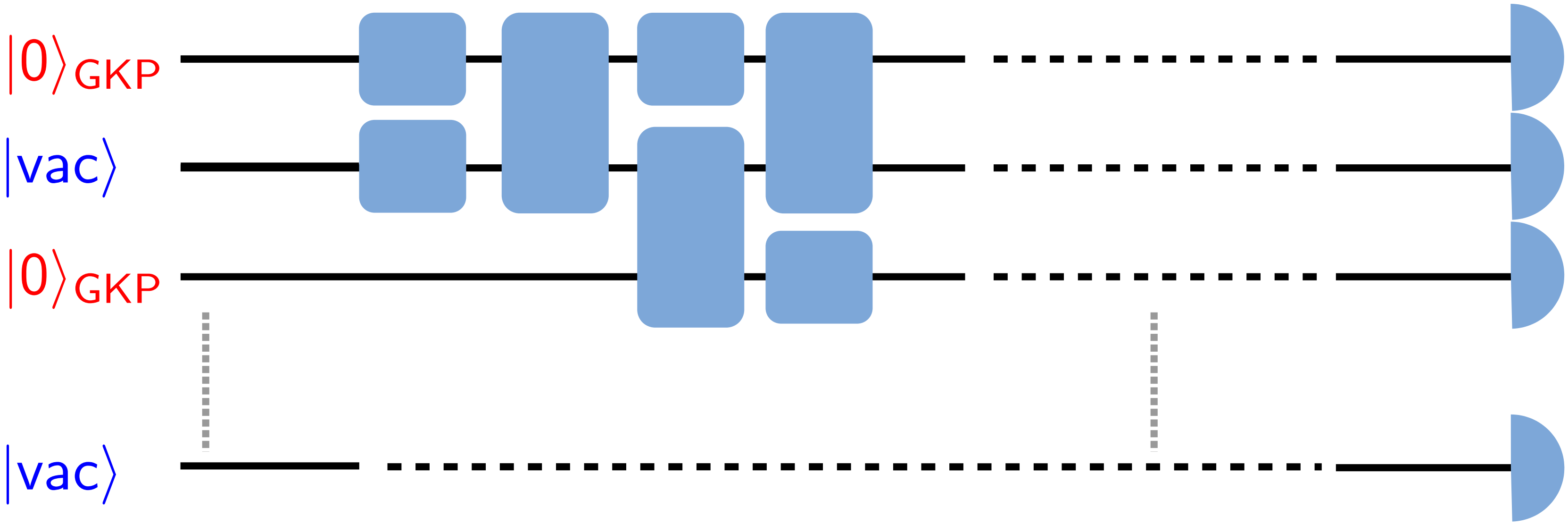

[Baragiola et al., PRL '19]

GKP states provide quantum advantage to otherwise simulatable circuits

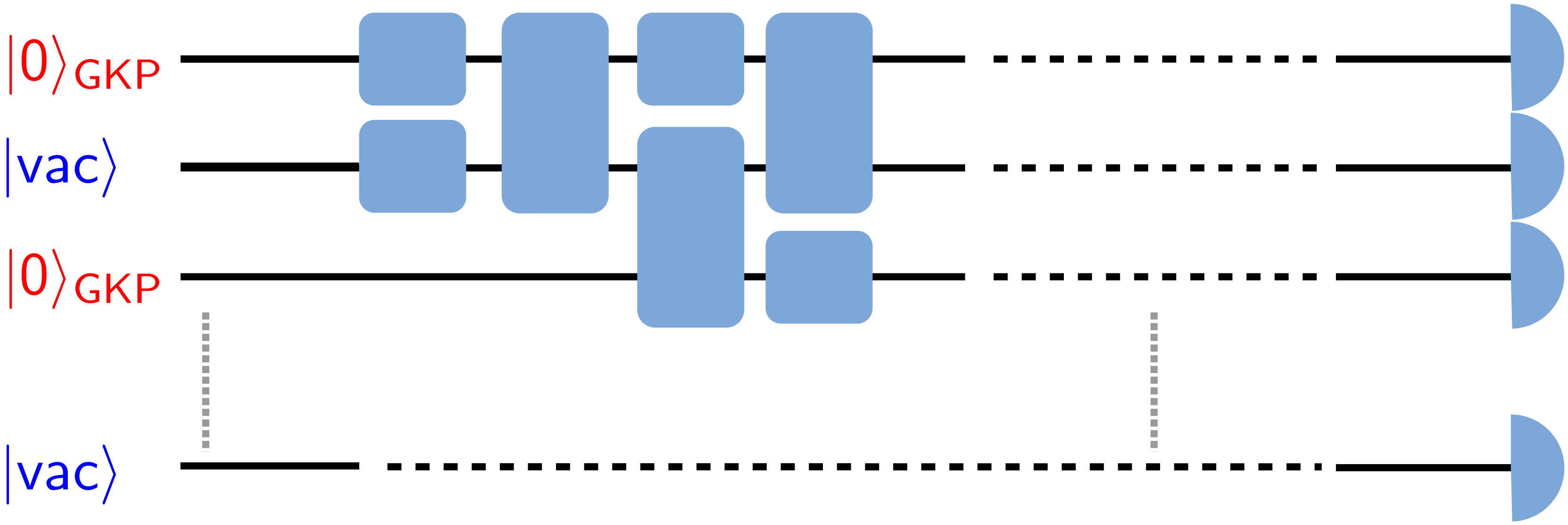

[Baragiola et al., PRL ‘19]

Vacuum provides quantum advantage to otherwise simulatable circuits

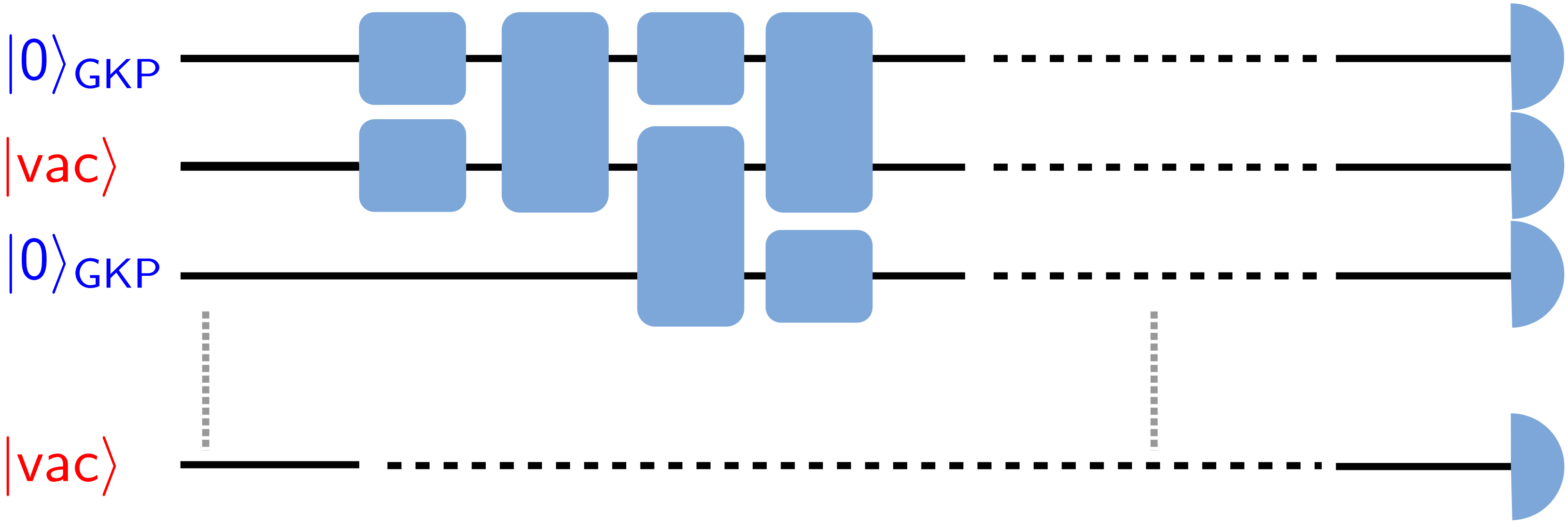

[Calcluth, AF, Ferrini, arXiv:2205.09781]

Why and how do we use infinite-dimensional systems?

Most quantum systems are infinite-dimensional
but we have to digitize them (bosonic codes)

What do we gain?

Excellent performances for noise-resilience and scalability

What is a genuine resource for quantum computational advantage?

Wigner negativity and classical simulatability

M Genoni, M Paris, F Albarelli (Milan)

S Blair, P McConnell, M Paternostro (Belfast)

G Ferrini, L García-Álvarez, C Calcluth, O Hanh

P Holmvall, F Quijandría, Y Zheng (Chalmers)

Available positions:

EIC Pathfinder 2 post-docs and 1 PhD
PRIN 2 post-docs

John Templeton Foundation
EPSRC
European Commission
MUR

A lot of the quantum world is "CVs"

Atomic ensembles

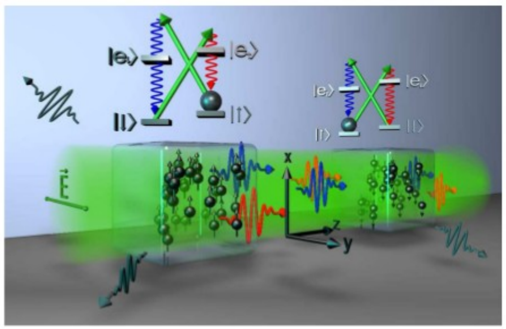

Trapped Ions

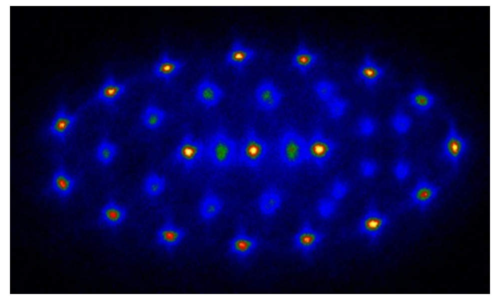

Opto- and
electro-mechanics

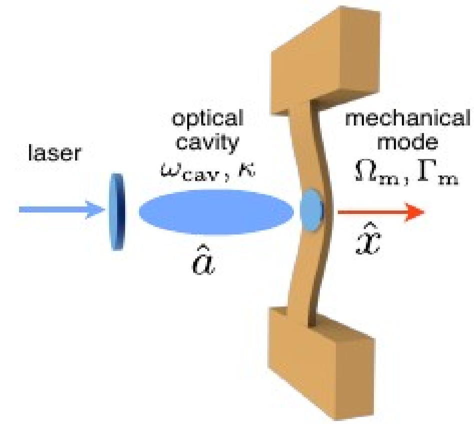

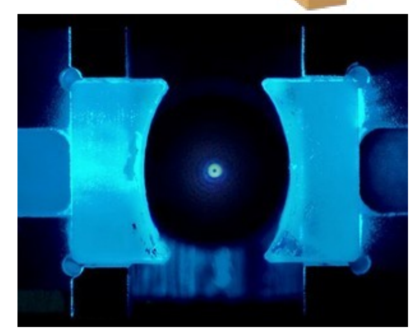

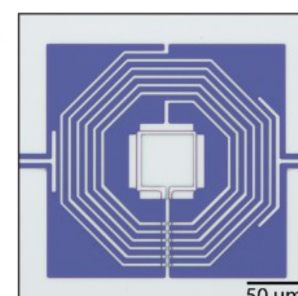

Cavity- and
Circuit-QED

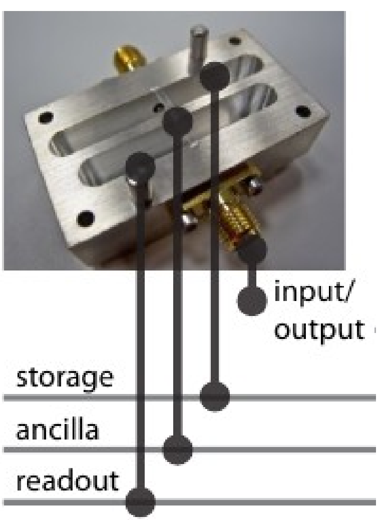

Photonics

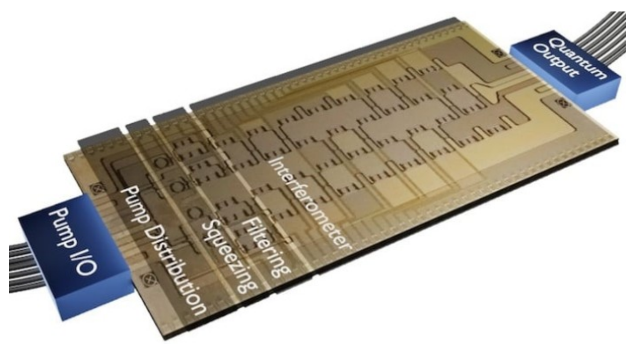

Digitizing CVs classical signals

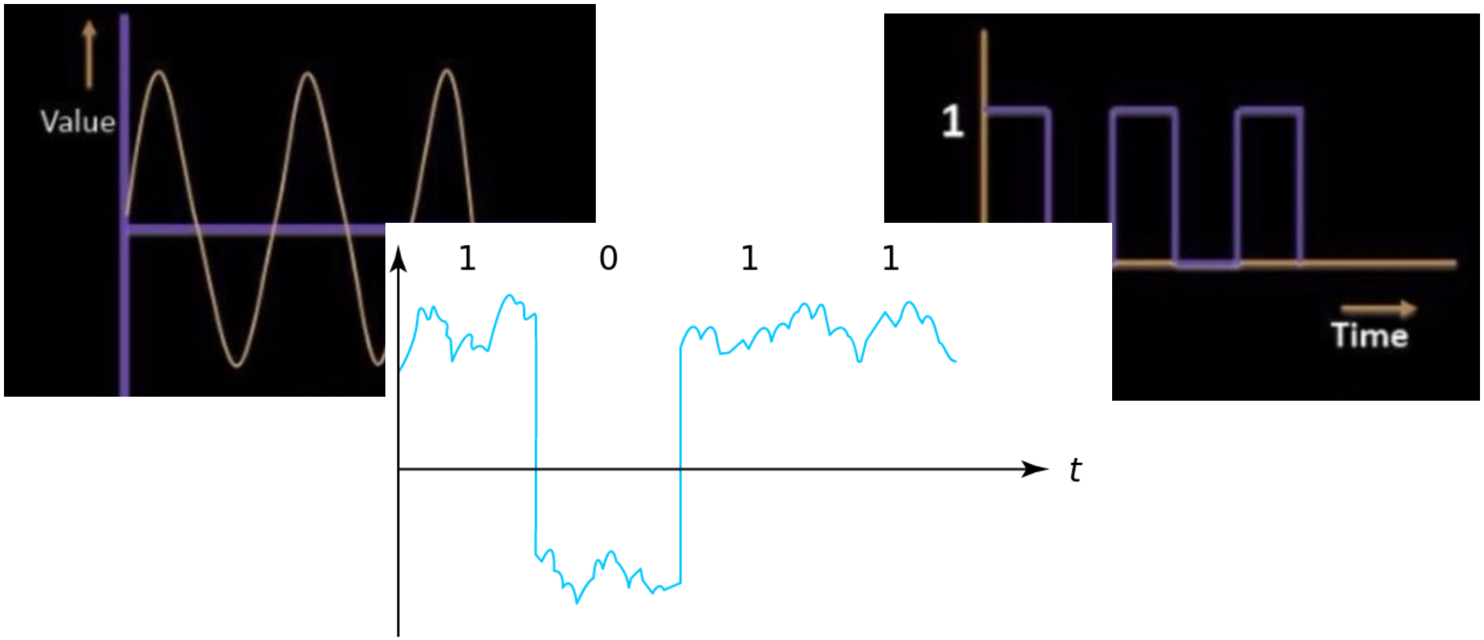

Digitizing CVs classical signals

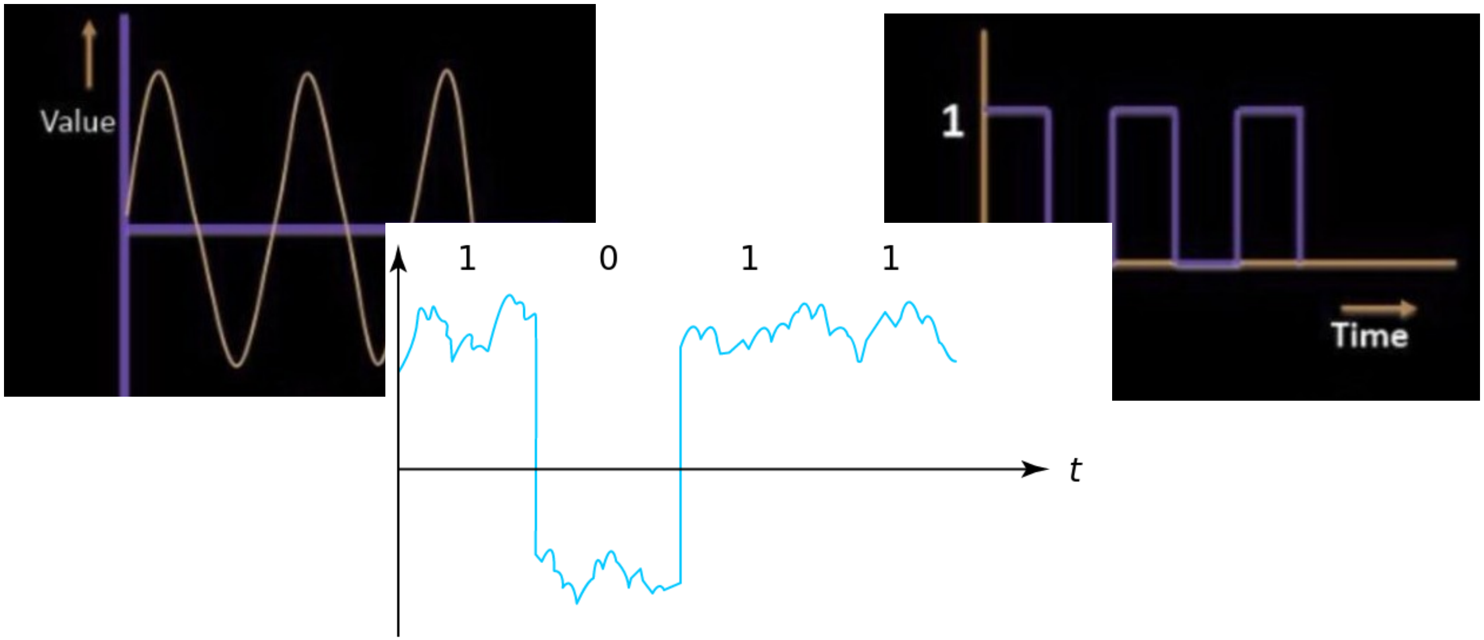

<u>Note</u>: for classical systems DVs are more the exception than the rule!

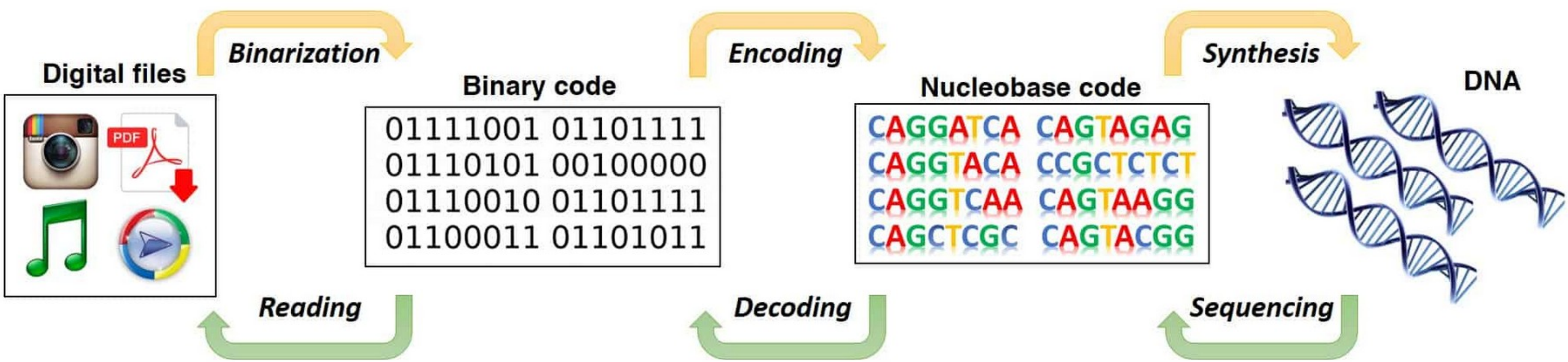

Digitizing quantum CVs: bosonic encoding

	Encoded qubits (wavefunction)	Pros	Cons
Fock state encoding	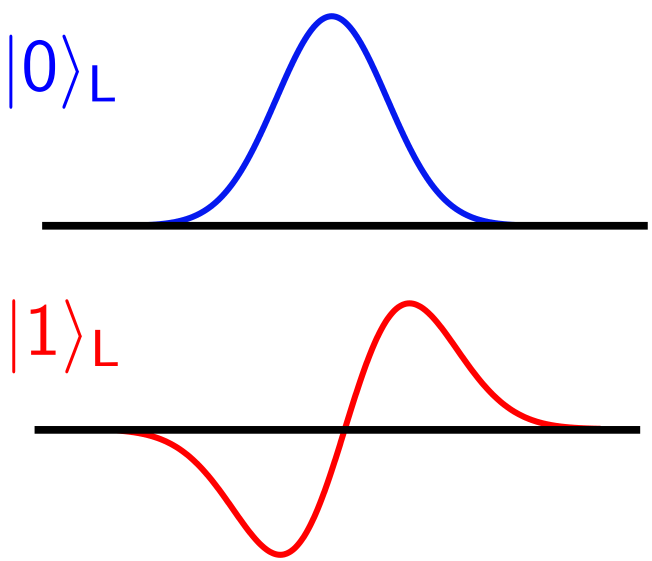	Experimentally "easy" to generate	Not resilient to noise (e.g., losses; small displacements break even/odd sym)
GKP state encoding **(n-locations at once)**	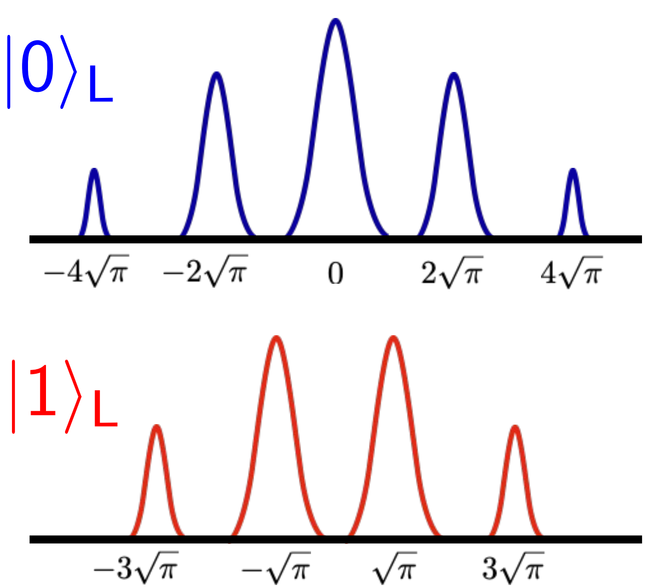	• Resilient to noise (losses, displacements) • Hardware efficient (fault-tolerant quantum computation)	"Difficult" to generate experimentally

Two pigeons with one stone: hardware efficiency and resilience to noise

Discrete variables

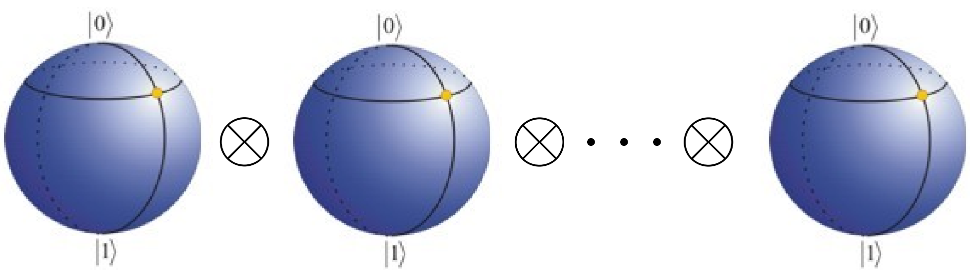

3-qubit repetition code

$$|0\rangle \rightarrow |0_L\rangle \equiv |000\rangle$$
$$|1\rangle \rightarrow |1_L\rangle \equiv |111\rangle$$

9-qubit Shor code

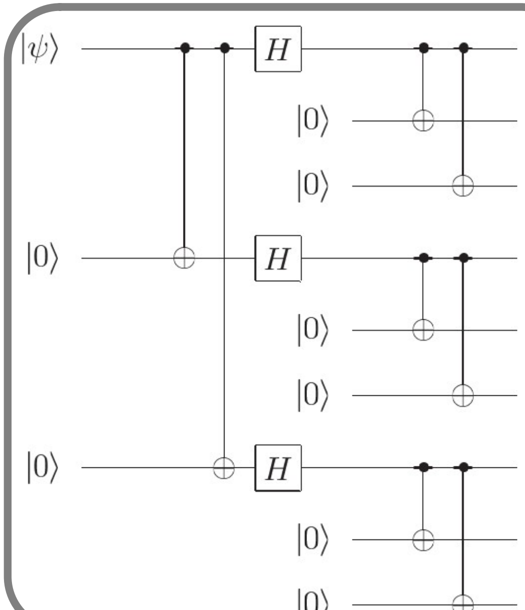

Continuous variables

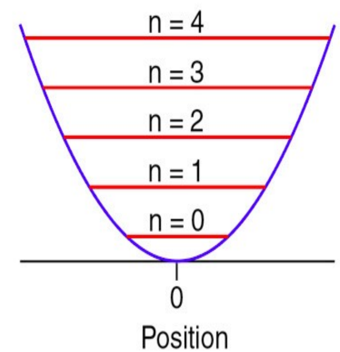

$$|\mathrm{cat}_{\mathrm{even}}\rangle \propto 2e^{-\frac{|\alpha|^2}{2}}\left(\frac{\alpha^0}{\sqrt{0!}}|0\rangle + \frac{\alpha^2}{\sqrt{2!}}|2\rangle + \ \ldots\right)$$
$$|\mathrm{cat}_{\mathrm{odd}}\rangle \propto 2e^{-\frac{|\alpha|^2}{2}}\left(\frac{\alpha^1}{\sqrt{1!}}|1\rangle + \frac{\alpha^3}{\sqrt{3!}}|3\rangle + \ \ldots\right)$$

Cat code

$$|0\rangle_L = \frac{1}{\sqrt{2}}(|0\rangle + |4\rangle)$$
$$|1\rangle_L = |2\rangle$$

Binomial code

CV codes (II): 4-headed cat code

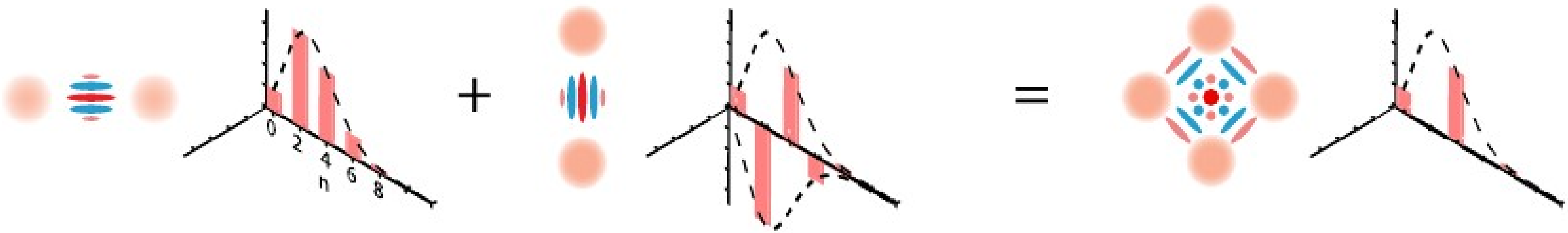

$$|\mathrm{cat_{even}}\rangle \propto \sum \frac{\alpha^{2n}}{\sqrt{(2n)!}}|2n\rangle \qquad |\mathrm{cat_{i,even}}\rangle \propto \sum \frac{(i\alpha)^{2n}}{\sqrt{(2n)!}}|2n\rangle \qquad |\mathrm{cat_{4,even}}\rangle \propto \sum \frac{(\alpha)^{4n}}{\sqrt{(4n)!}}|4n\rangle$$

$$|\mathrm{cat_{4,even}}\rangle \propto \frac{(\alpha)^{0}}{\sqrt{(0)!}}|0\rangle + \frac{(\alpha)^{4}}{\sqrt{(4)!}}|4\rangle + \frac{(\alpha)^{8}}{\sqrt{(8)!}}|8\rangle + \dots$$

Extending the lifetime of a quantum bit with error correction in superconducting circuits

Nature 536, 441–445 (2016) Ofek, N., Petrenko, A., Heeres, R. *et al.*

(a)

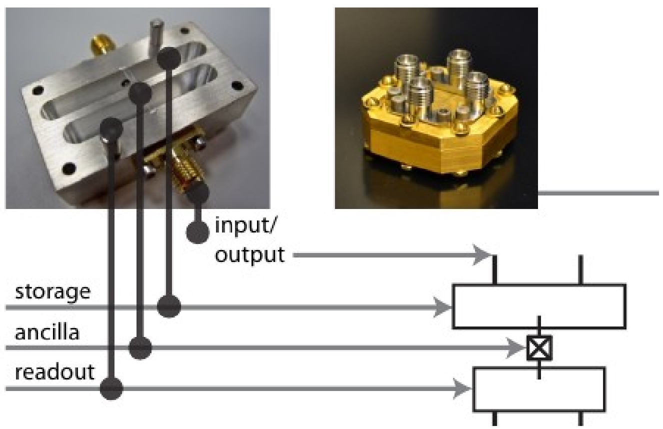

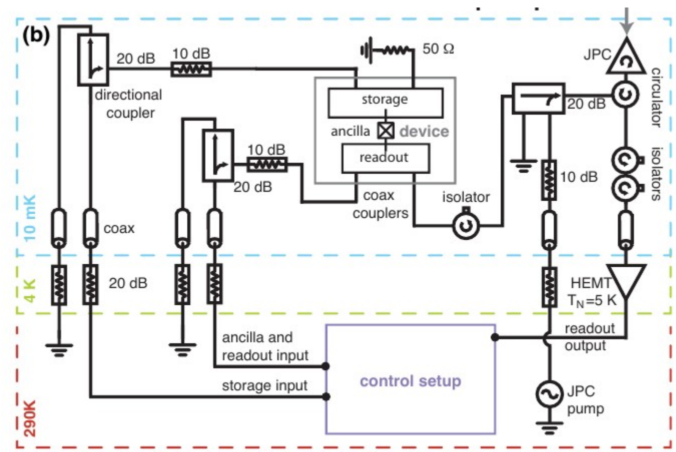

Photon loss can be corrected (code cycle: monitoring plus mapping to transmon with the proper mapping function depending on the syndrome monitoring):

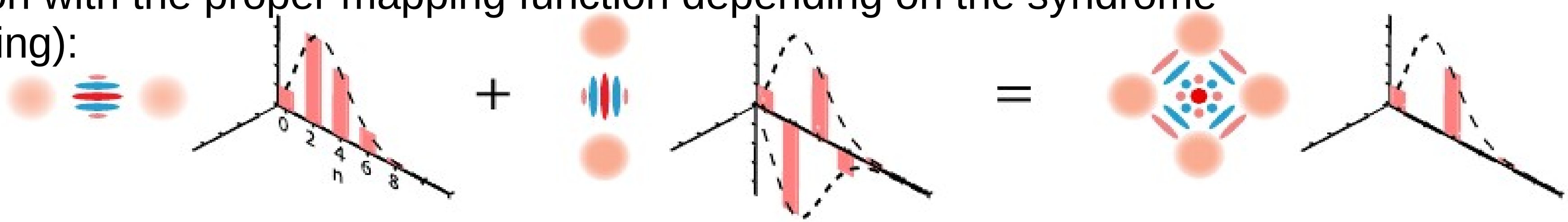

$$|0_L^+\rangle = \frac{1}{\sqrt{2}}(|\alpha\rangle + |-\alpha\rangle) = \sqrt{2}e^{-\frac{|\alpha|^2}{2}} \sum_{n=0} \frac{\alpha^{2n}}{\sqrt{(2n)!}} |2n\rangle$$

$$|1_L^+\rangle = \frac{1}{\sqrt{2}}(|i\alpha\rangle + |-i\alpha\rangle) = \sqrt{2}e^{-\frac{|\alpha|^2}{2}} \sum_{n=0} \frac{(i\alpha)^{2n}}{\sqrt{(2n)!}} |2n\rangle$$

$$|X_L^+\rangle = \frac{1}{\sqrt{2}}(|C_\alpha^+\rangle + |C_{i\alpha}^+\rangle) = 2e^{-\frac{|\alpha|^2}{2}} \sum_{n=0} \frac{\alpha^{4n}}{\sqrt{(4n)!}} |4n\rangle$$

PHYSICAL REVIEW A, VOLUME 64, 012310

Encoding a qubit in an oscillator

Daniel Gottesman,[1,2,*] Alexei Kitaev,[1,†] and John Preskill[3,‡]

(Received 9 August 2000; published 11 June 2001)

$$|0\rangle_L = \sum_{j=-\infty}^{\infty} |2j\sqrt{\pi}\rangle_q$$

$$|1\rangle_L = \sum_{j=-\infty}^{\infty} |(2j+1)\sqrt{\pi}\rangle_q$$

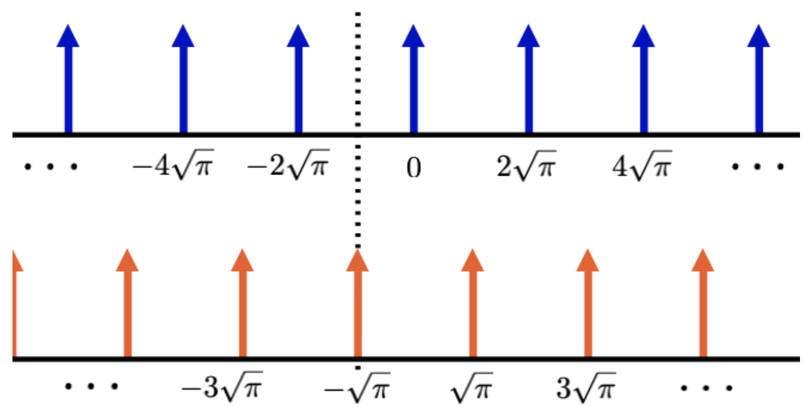

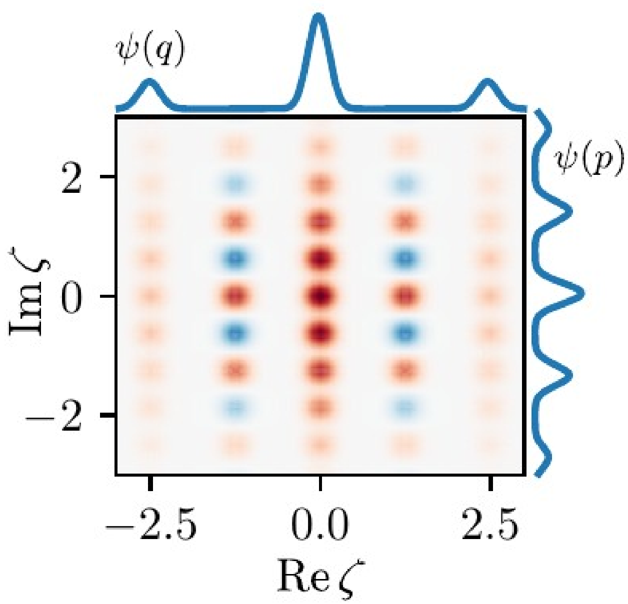

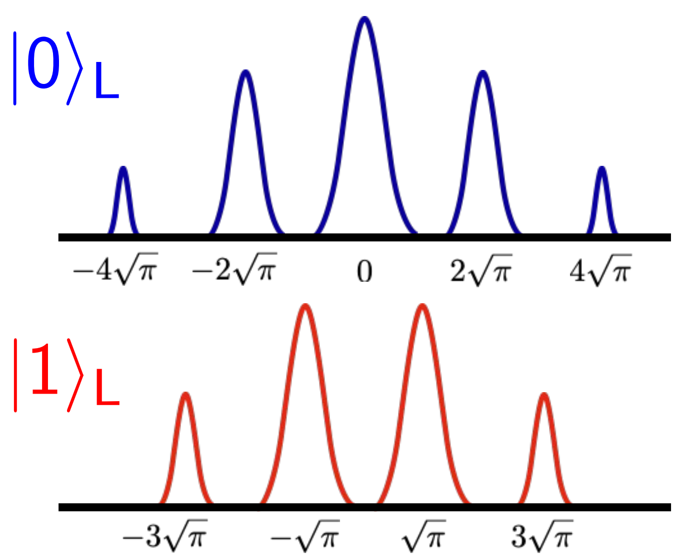

As long as the overlap is small, errors can be corrected for.

Encoding a qubit in a trapped-ion mechanical oscillator

C. Flühmann, T. L. Nguyen, M. Marinelli, V. Negnevitsky, K. Mehta & J. P. Home

Nature 566, 513–517 (2019) | Cite this article

$$\hat{H}_{\mathrm{SDF}} = \eta\hbar\Omega\hat{\sigma}_x(\hat{a}e^{i\Delta\phi/2} + \hat{a}^\dagger e^{-i\Delta\phi/2})/2$$

$$\hat{\mathcal{D}}(\alpha(t)\hat{\sigma}_x/2), \text{ where } \alpha(t) = ie^{i\Delta\phi/2}\eta\Omega t$$

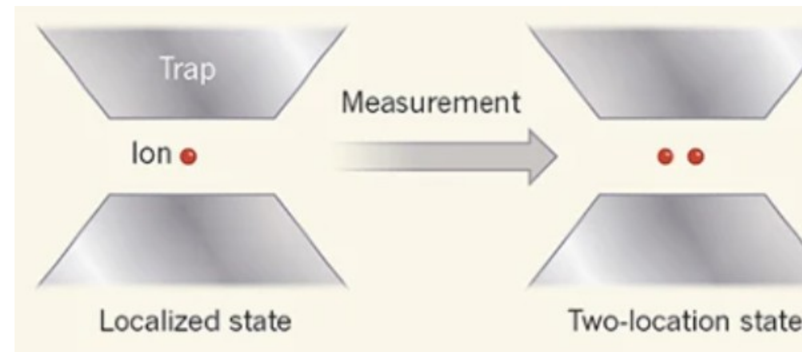

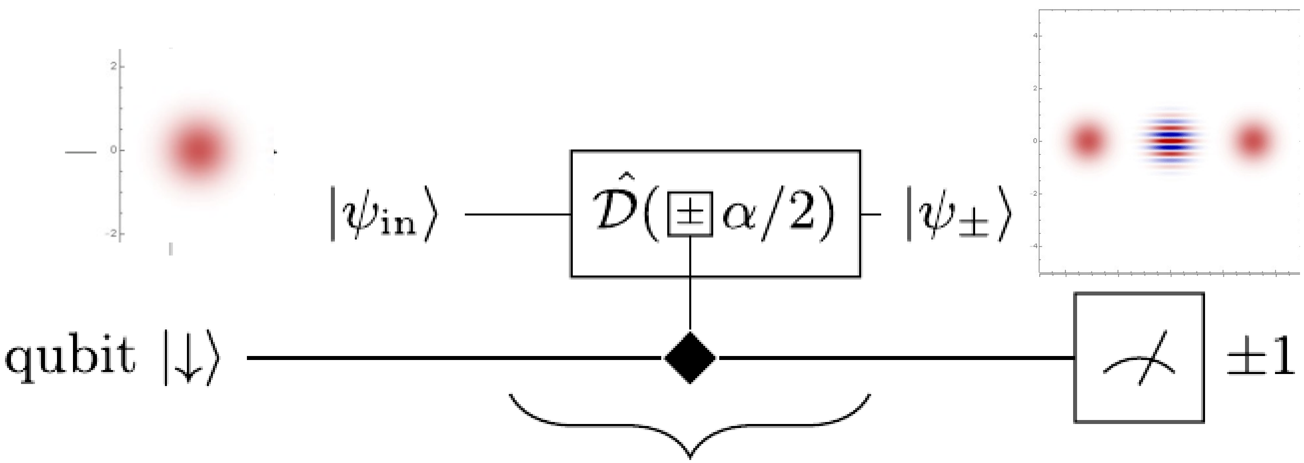

$$\text{SDF:} \quad |+\rangle|\psi_{\mathrm{in}}\rangle \rightarrow |+\rangle\hat{\mathcal{D}}(+\alpha/2)|\psi_{\mathrm{in}}\rangle,$$
$$|-\rangle|\psi_{\mathrm{in}}\rangle \rightarrow |-\rangle\hat{\mathcal{D}}(-\alpha/2)|\psi_{\mathrm{in}}\rangle$$

[Fluhmann, PRX 8, 021001 (2018)]

Associated Content

Promising ways to encode and manipulate quantum information

Alessandro Ferraro

Nature | **News & Views** | 27 Feb 2019

Resourcefulness comparison (at fixed energy)

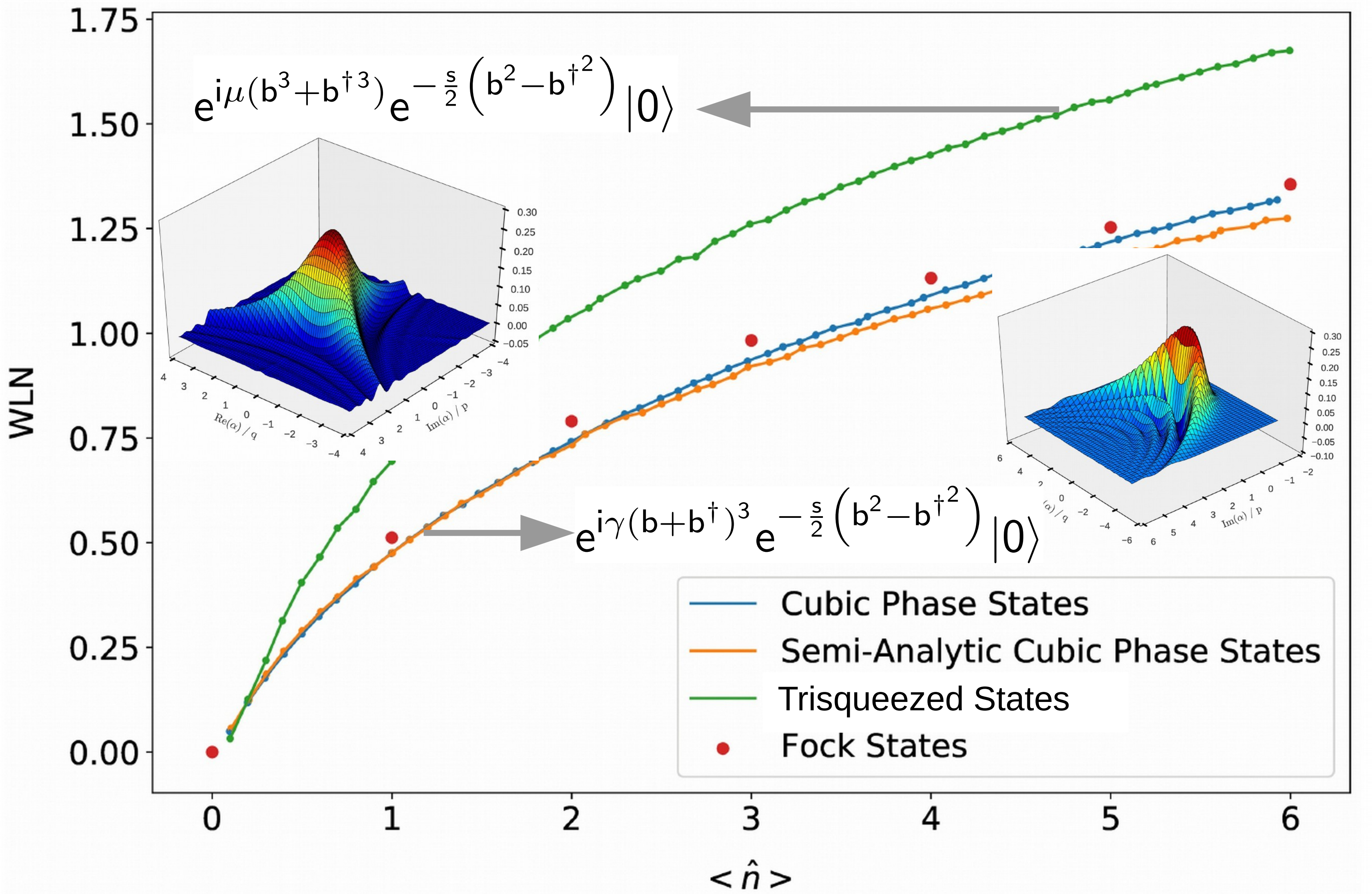

Fock states are not the most resourceful states at fixed energy

[McConnell, AF, Puebla, arXiv:2209.07958]

Resource conversion: Trisqueezed to Cubic-Phase State

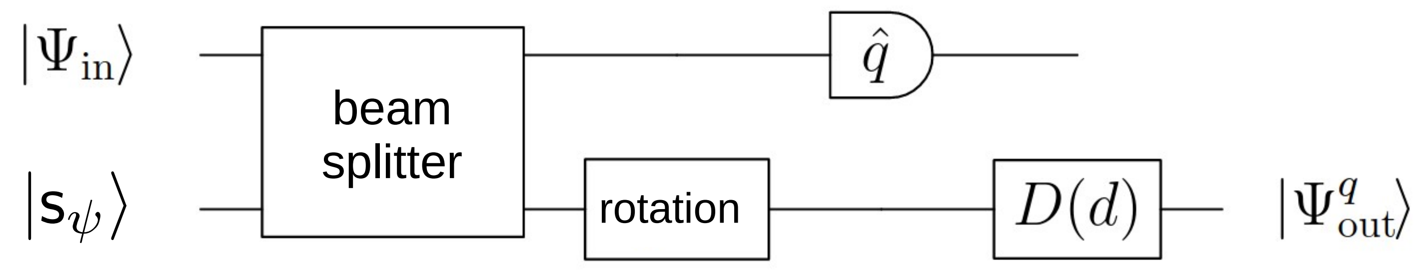

[Zheng, Hahn, Stadler, Holmvall, Qijandría, AF and Ferrini, PRXQ 2021]

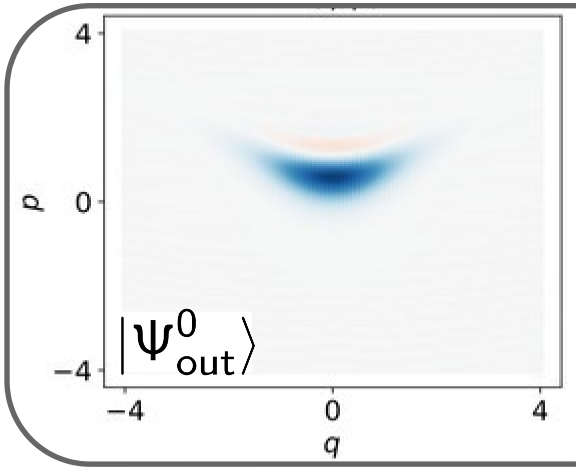

Input:

$t = 0.1$

Target:

$\gamma = 0.1558$

$s = 5\text{dB}$

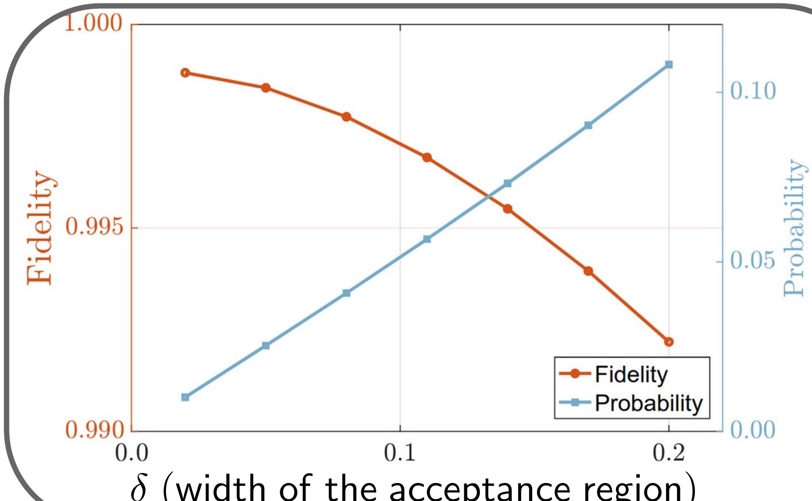

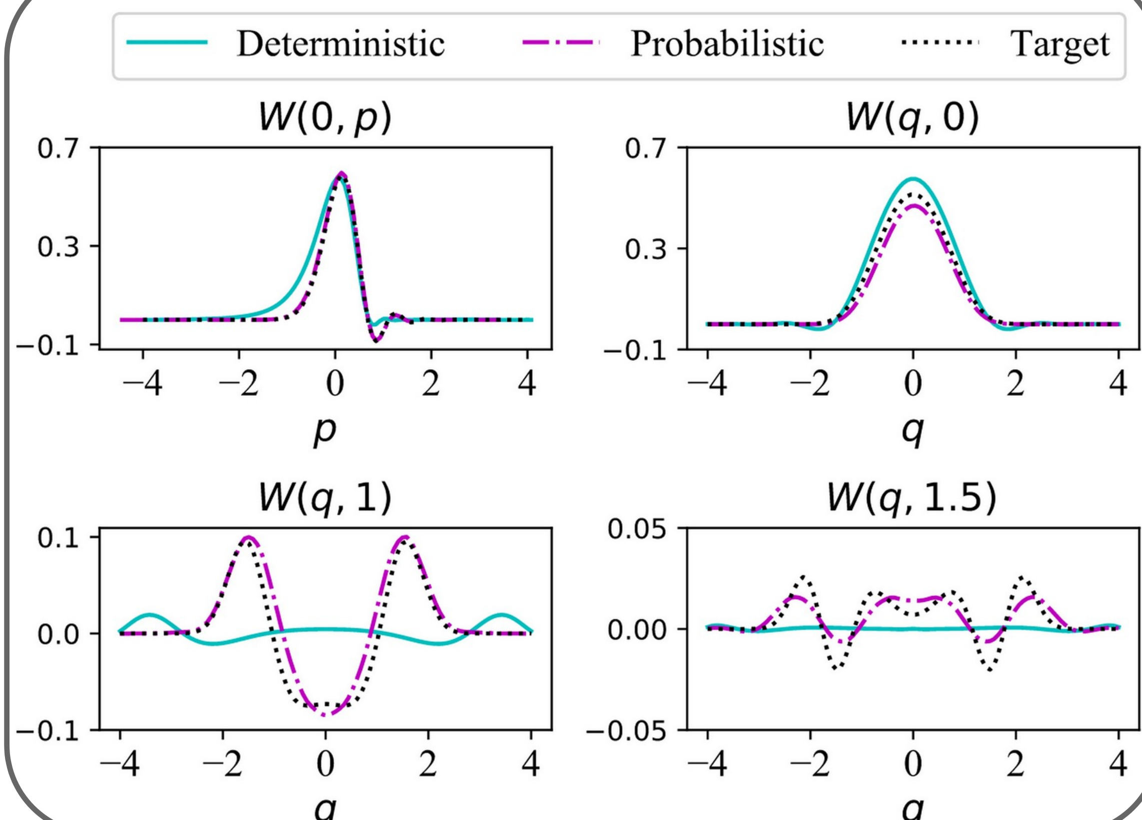

Sweet spot: F = 99.6% with p = 7%

Resource conversion: photon-subtracted/added and cat states

Photon-subtracted/added squeezed state

$$\begin{cases} \frac{1}{\mathcal{N}}\ \hat{a}^N|s\rangle, & \text{if } N<0 \\ \frac{1}{\mathcal{N}'}\ (\hat{a}^\dagger)^N|s\rangle, & \text{if } N>0 \end{cases}$$

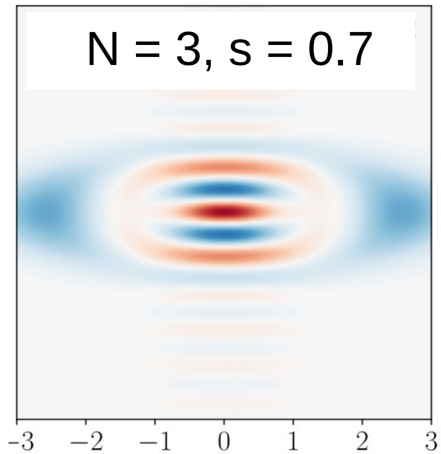

Cat states $(\mathrm{N}=1): \mu = 0(\mathrm{even}), 1(\mathrm{odd})$

$$\frac{1}{\sqrt{\mathcal{N}}}\sum_{m=0}^{2N-1}(-1)^{\mu\cdot m}e^{i\frac{m\pi}{N}\hat{n}}|\alpha\rangle$$

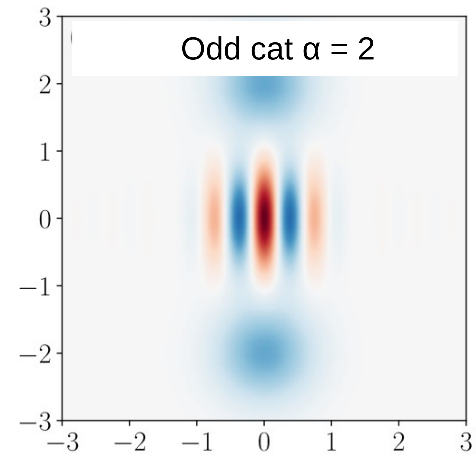

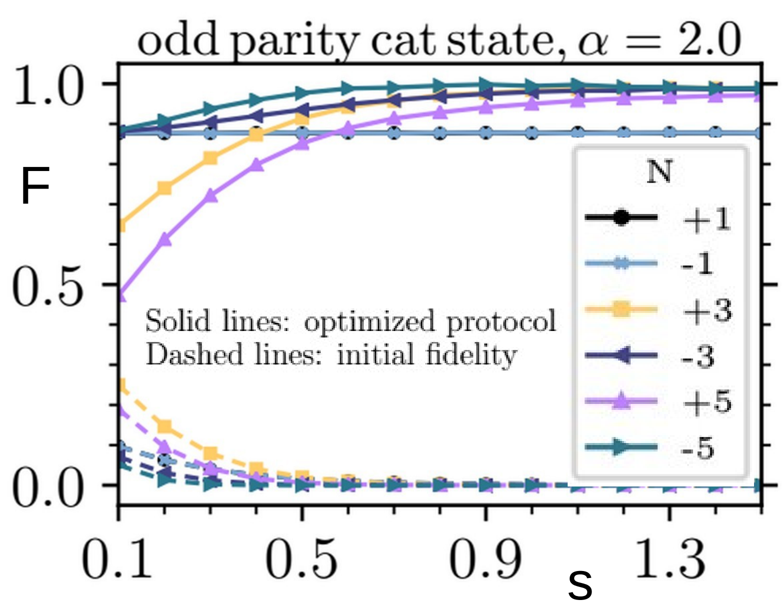

High-fidelity conversions from photon-subtracted/added states to large-amplitude cat states can be achieved for optimized N and squeezing (*rotation + squeezing protocols*)

[Hahn, Holmvall, Stadler, Ferrini, AF, PRA 2022]

Many resource states in labs

PRX QUANTUM **3,** 030301 (2022)

Robust Preparation of Wigner-Negative States with Optimized SNAP-Displacement Sequences

Marina Kudra,[1,*] Mikael Kervinen,[1] Ingrid Strandberg,[1] Shahnawaz Ahmed,[1] Marco Scigliuzzo,[1] Amr Osman,[1] Daniel Pérez Lozano,[1] Mats O. Tholén,[2] Riccardo Borgani,[2] David B. Haviland,[2] Giulia Ferrini,[1] Jonas Bylander,[1] Anton Frisk Kockum,[1] Fernando Quijandría,[1,§] Per Delsing,[1,†] and Simone Gasparinetti[1,‡]

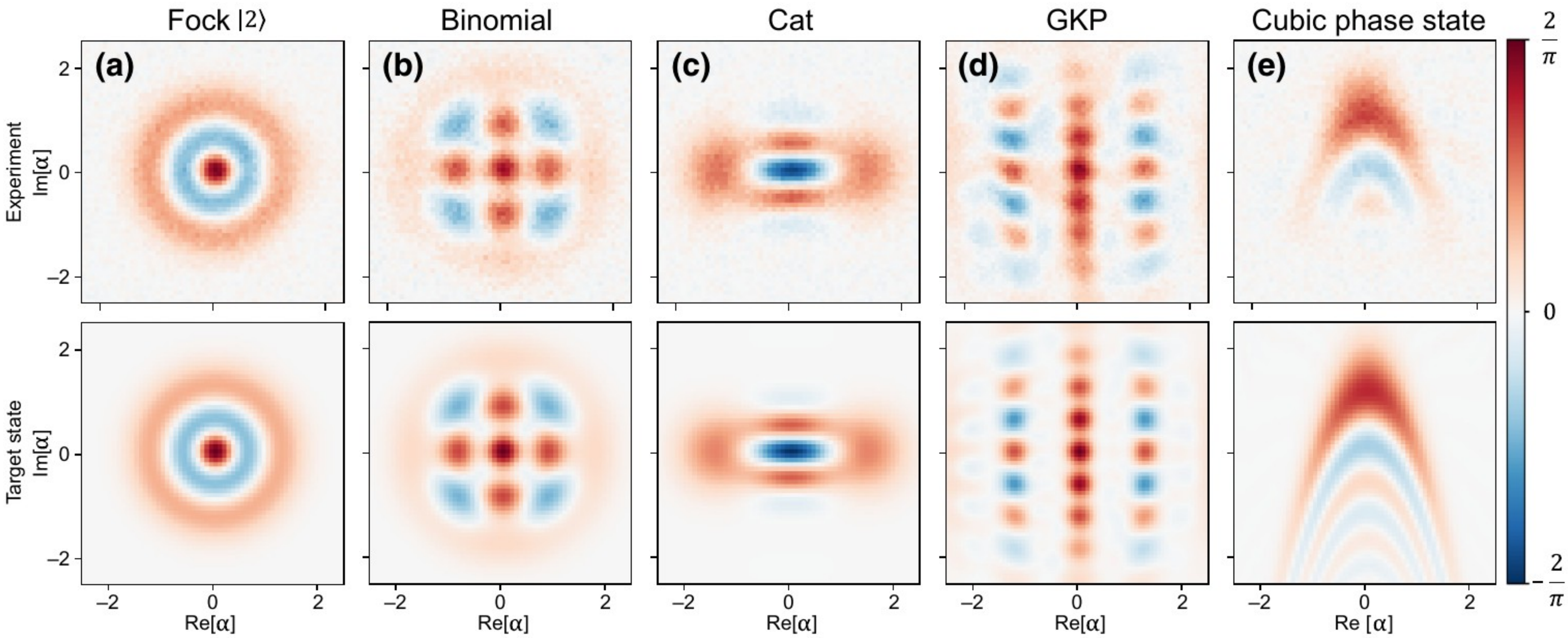

PHYSICAL REVIEW A **92**, 040303(R) (2015)

Universal control of an oscillator with dispersive coupling to a qubit

Stefan Krastanov,[1] Victor V. Albert,[1] Chao Shen,[1] Chang-Ling Zou,[1,2] Reinier W. Heeres,[1] Brian Vlastakis,[1] Robert J. Schoelkopf,[1] and Liang Jiang[1]

$$\hat{H} = \hat{H}_0 + \hat{H}_1 + \hat{H}_2,$$

with a dispersively coupled qubit and oscillator

$$\hat{H}_0 = \omega_q |e\rangle\langle e| + \omega_c \hat{n} - \chi |e\rangle\langle e| \hat{n},$$

time-dependent drive of the oscillator,

$$\hat{H}_1 = \epsilon(t) e^{i\omega_c t} \hat{a}^\dagger + \text{H.c.},$$

and time-dependent drive of the qubit,

$$\hat{H}_2 = \Omega(t) e^{i\omega_q t} |e\rangle\langle g| + \text{H.c.}$$

$$\hat{D}(\alpha) = \exp(\alpha \hat{a}^\dagger - \alpha^* \hat{a})$$

$$\Omega(t) = \sum_n \Omega_n(t) e^{i(\omega_q - \chi n)t}$$

$$\hat{S}(\vec{\theta}) = \sum_{n=0}^{\infty} e^{i\theta_n} |n\rangle\langle n|$$

(decoupled form the qubit)

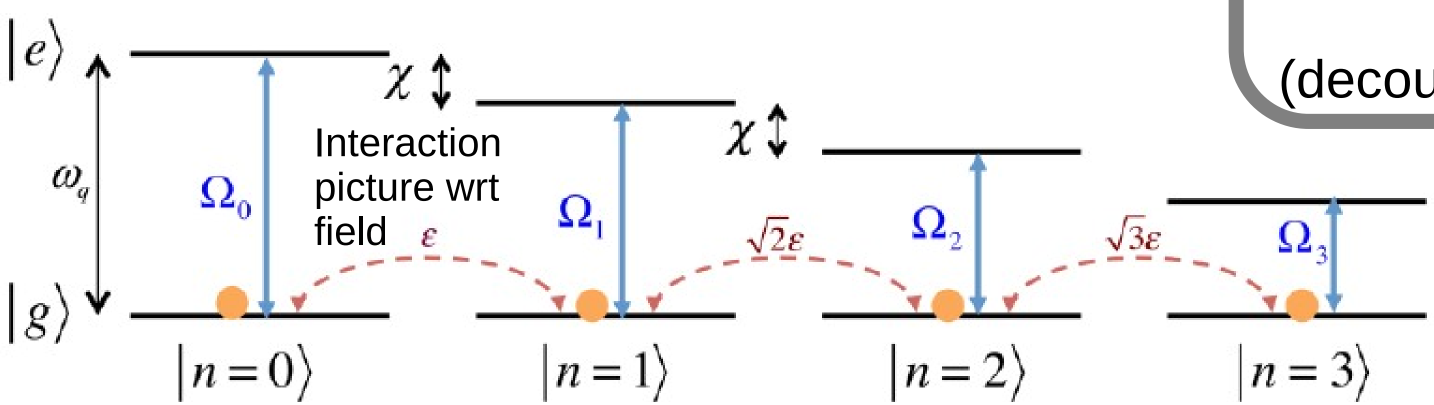

Selective Number-dependent Arbitrary Phase gate (eg, F, Kerr,...)

arXiv > quant-ph > arXiv:2004.14256

Efficient cavity control with SNAP gates

Thomas Fösel, Stefan Krastanov, Florian Marquardt, Liang Jiang

$$\hat{S}(\vec{\theta}) = \sum_{n=0}^{\infty} e^{i\theta^{(n)}} |n\rangle\langle n|$$

$$\hat{D}(\alpha) = \exp(\alpha \hat{a}^{\dagger} + \alpha^{*}\hat{a}).$$

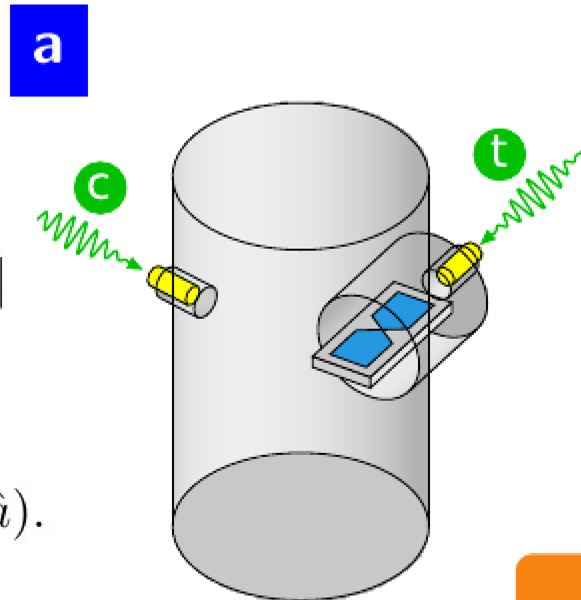

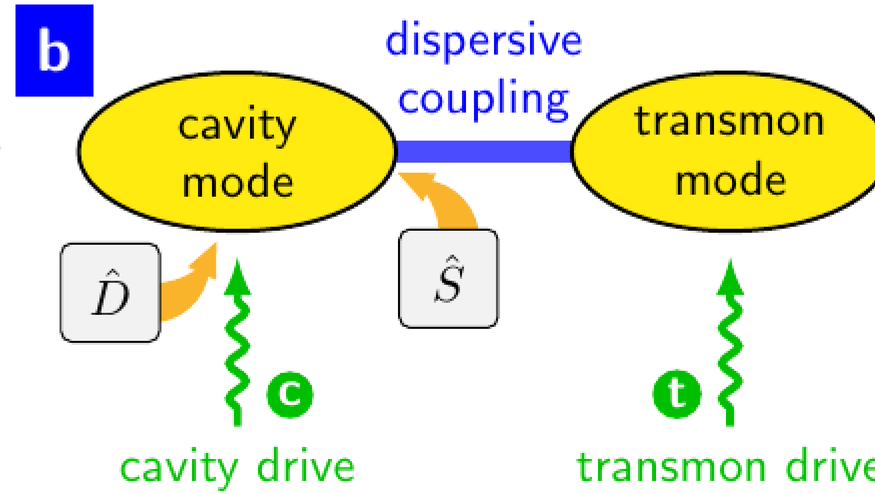

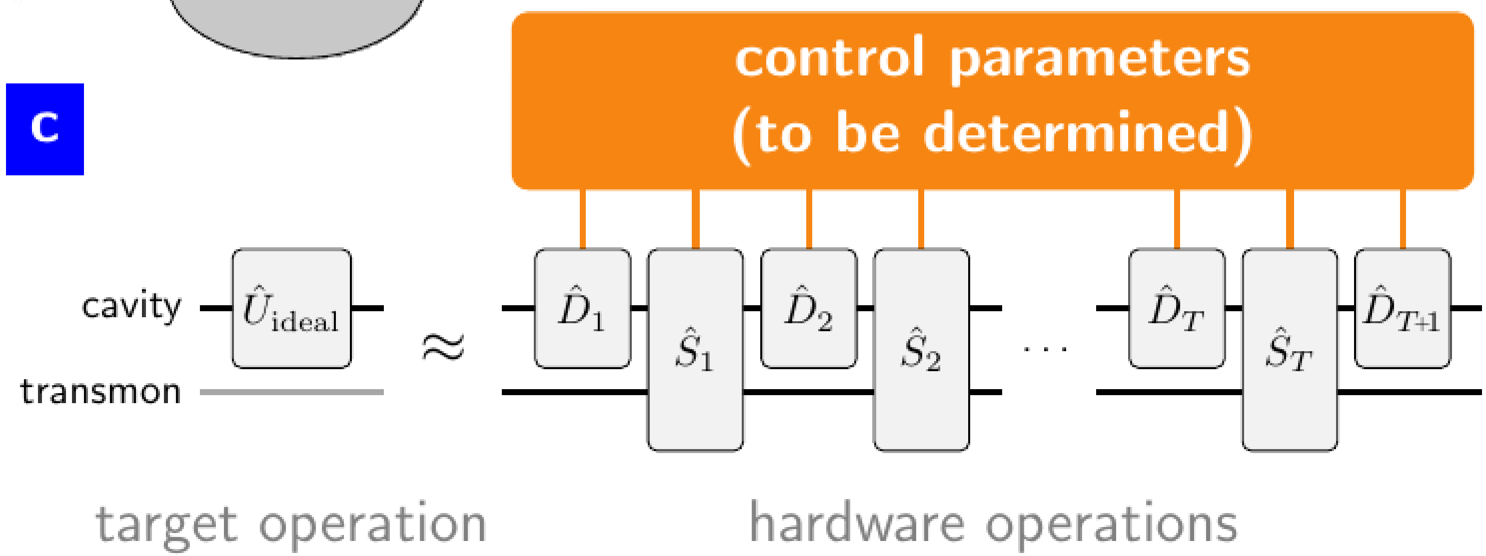

$$\hat{U} = \hat{D}(\alpha_{T+1}) \cdot \hat{S}(\vec{\theta}_T) \cdot \hat{D}(\alpha_T) \cdot \ldots \cdot \hat{S}(\vec{\theta}_2) \cdot \hat{D}(\alpha_2) \cdot \hat{S}(\vec{\theta}_1) \cdot \hat{D}(\alpha_1)$$

Universal gate set, with typically short sequences arXiv > quant-ph > arXiv:2211.09116

Real-time quantum error correction beyond break-even

V. V. Sivak, A. Eickbusch, B. Royer, S. Singh, I. Tsioutsios, S. Ganjam, A. Miano, B. L.
Ding, L. Frunzio, S. M. Girvin, R. J. Schoelkopf, M. H. Devoret

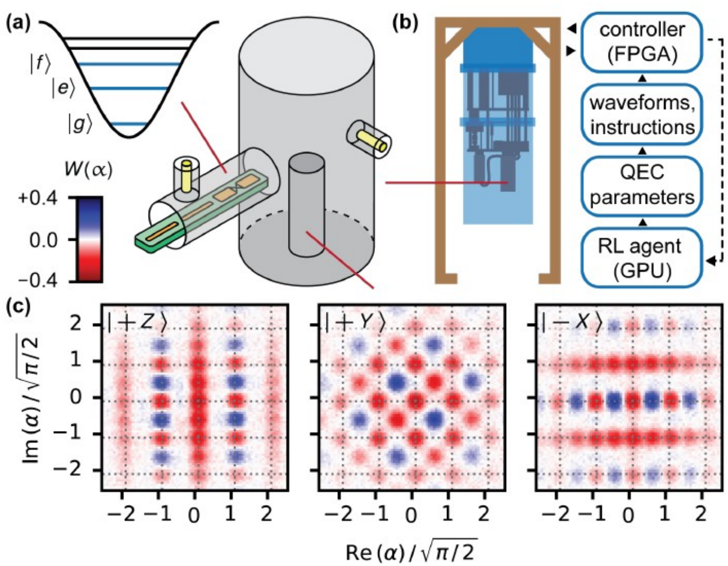

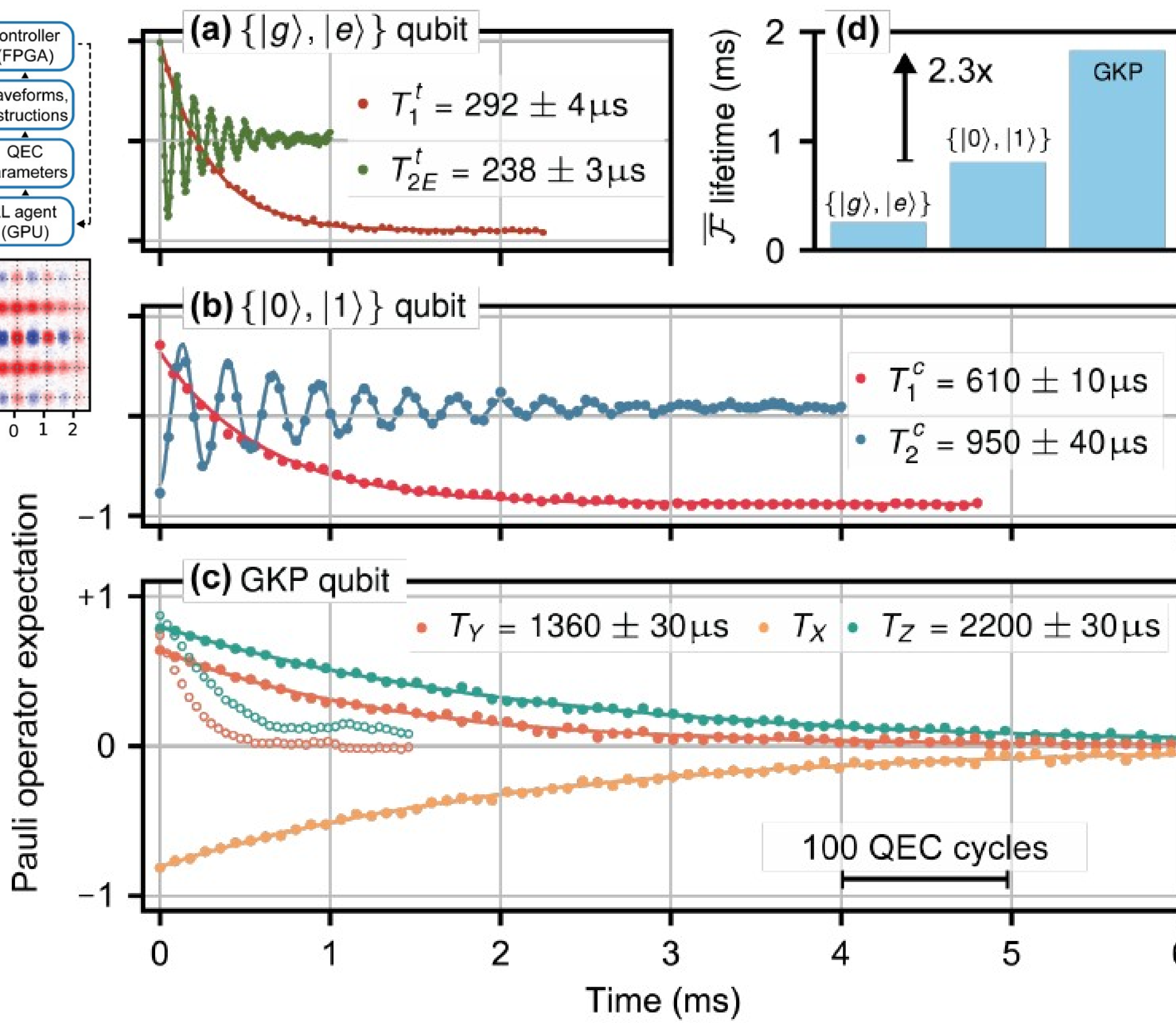

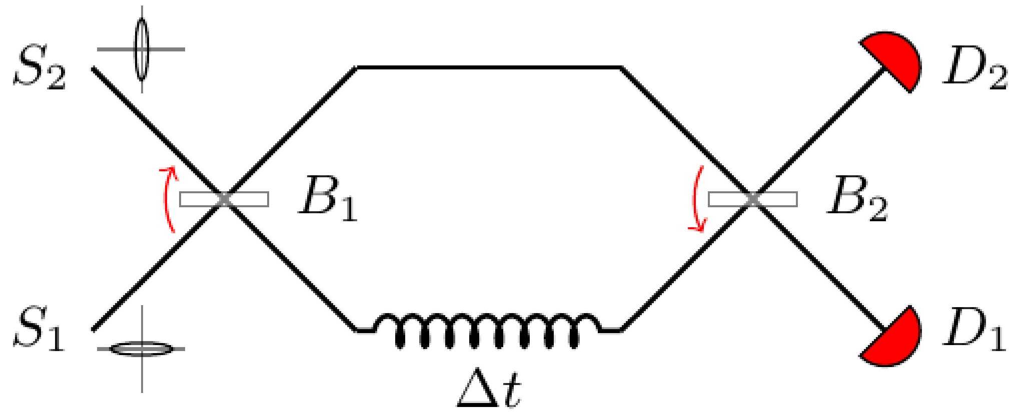

FIG. 2. Temporal-mode GPEPS construction of a CV quantum wire using passive squeezing and linear optics. Two single-mode squeezers S_1 and S_2 generate vacuum $\hat{p}$- and $\hat{q}$-squeezed pulses of light (respectively, as shown) at regular intervals Δt. These pass through a simple 50:50 beamsplitter B_1, resulting in a two-mode squeezed state. (Red arrows point from the first node to the second in Eq. (18) for each beamsplitter.) The delay loop in the bottom line delays the bottom mode by Δt, allowing it to match up with the top mode of the subsequent pair emerging from B_1, resulting schematically in the graph shown in Eq. (21). The second 50:50 beamsplitter B_2 implements sequentially each of the transformations indicated by the red arrows, resulting in the final graph of Eq. (22). These pulses

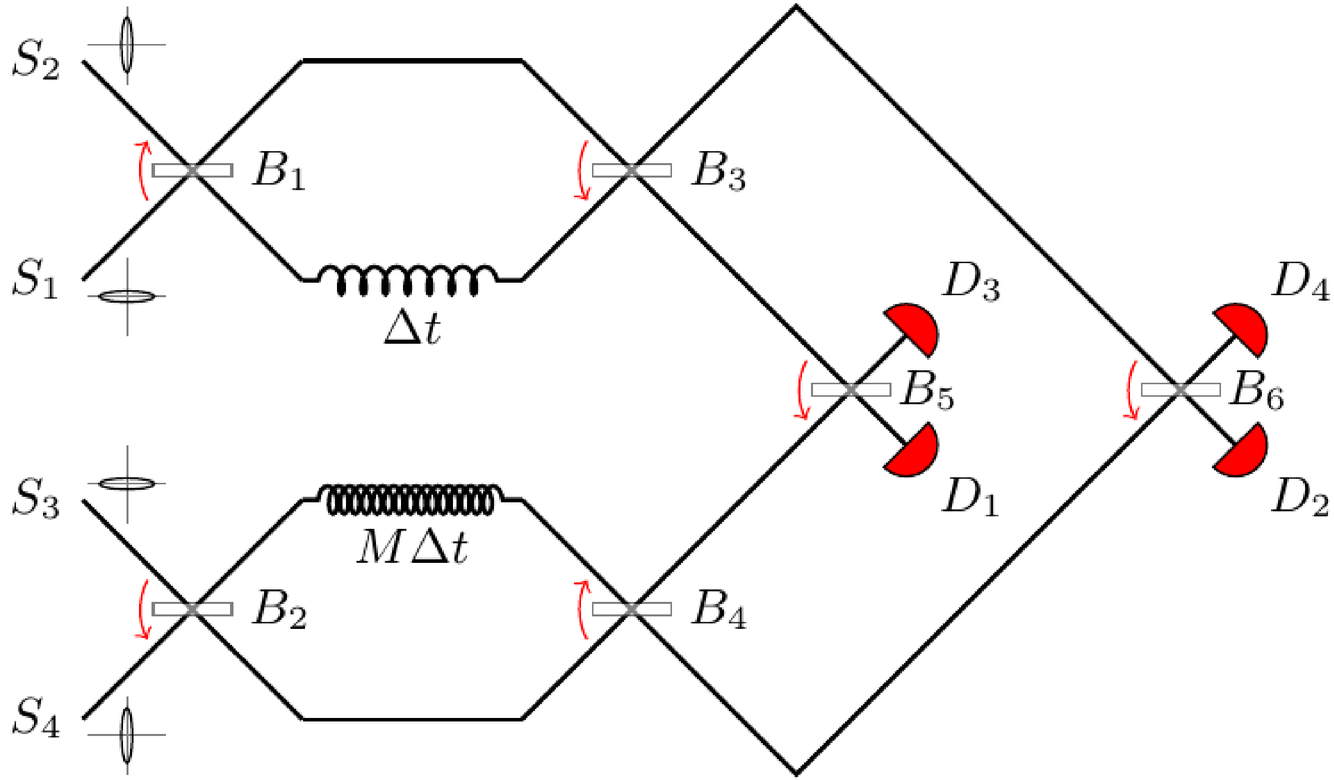

FIG. 4. Temporal-mode GPEPS construction of a square-lattice CV cluster state using passive squeezing and linear optics. Two copies of the quantum-wire setup from Figure 2 are used to generate the lattice. The upper one has the ordinary delay of Δt and corresponds to the vertical links in Figure 3 (top). The longer delay of $M\Delta t$ in the lower one gives the second threading of the wire and corresponds to the horizontal links in Figure 3 (top). Beamsplitters B_3 and B_4 implement the transformations indicated by red arrows in Eq. (26). (Red arrows point from the first node to the second in Eq. (18) for each beamsplitter.) Following this, the 50:50 beamsplitters B_5 and B_6 implement the transformations indicated by red arrows in Eq. (27), eventually resulting in the state with graph $\mathbf{Z}$ from Eq. (25). The

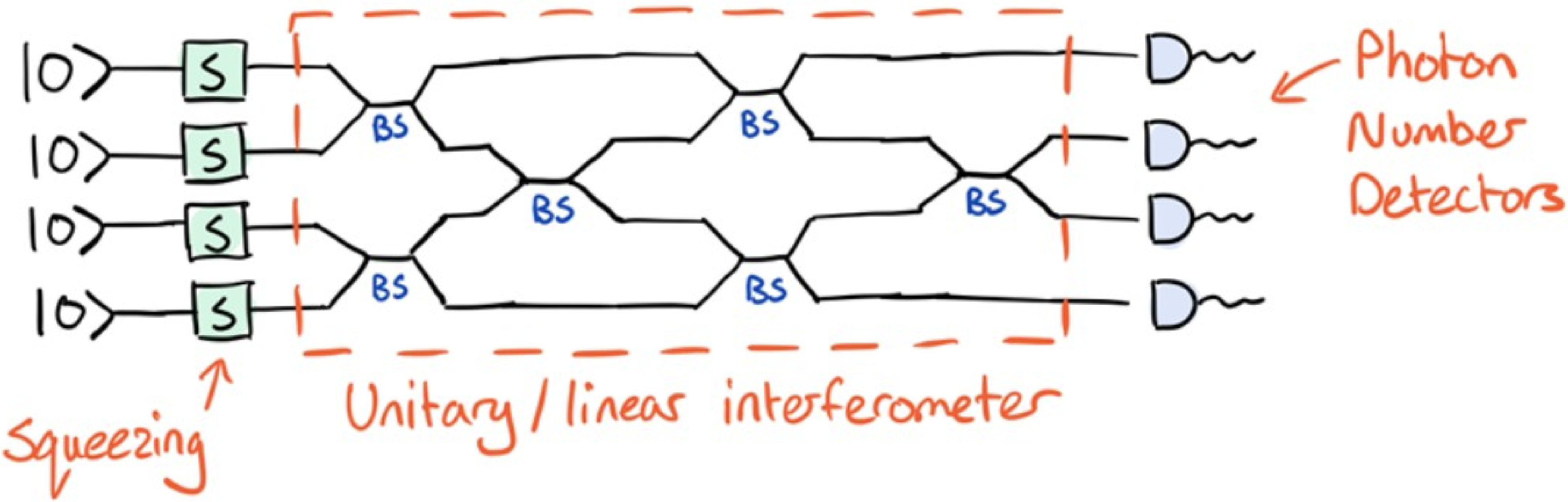

|0⟩
|0⟩
|0⟩
|0⟩
S
S
S
S
BS
BS
BS
BS
BS
BS
Photon Number Detectors
Squeezing
Unitary / linear interferometer

Blueprint for a Scalable Photonic Fault-Tolerant Quantum Computer

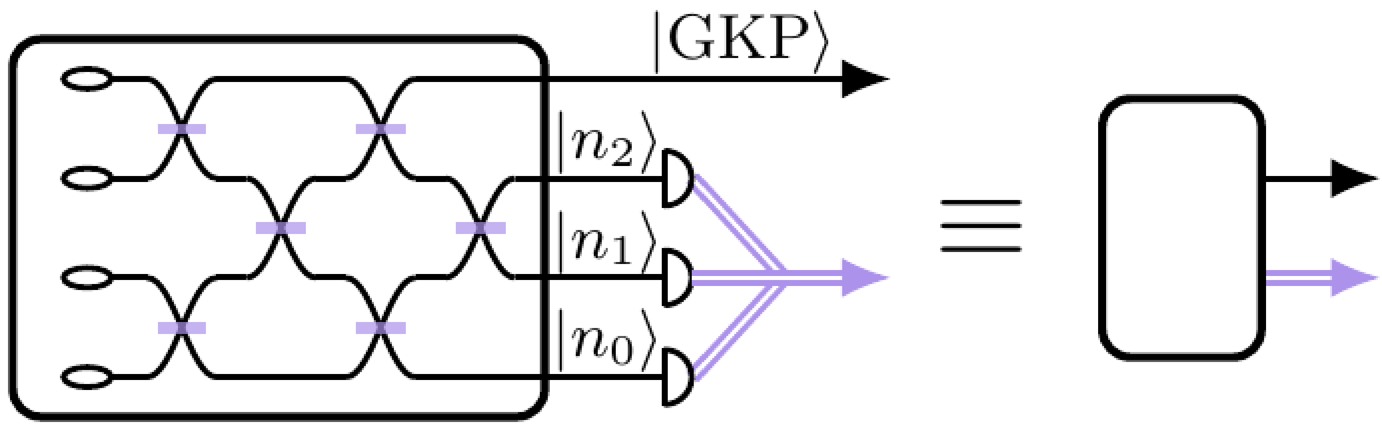

Figure 1: GBS devices for state preparation. (left) A single integrated photonic device implementing GBS-based preparation of non-Gaussian states based on the schemes presented in Refs. [27–30]. The emitted light from one output port is in a chosen non-Gaussian state subject to obtaining the correct click pattern $\{n_i\}$ at the PNR detectors connected to the remaining output ports. The double purple lines represent classical logic, which is used to trigger a switch on the emitted port. (right) A simplified representation of a single GBS device.

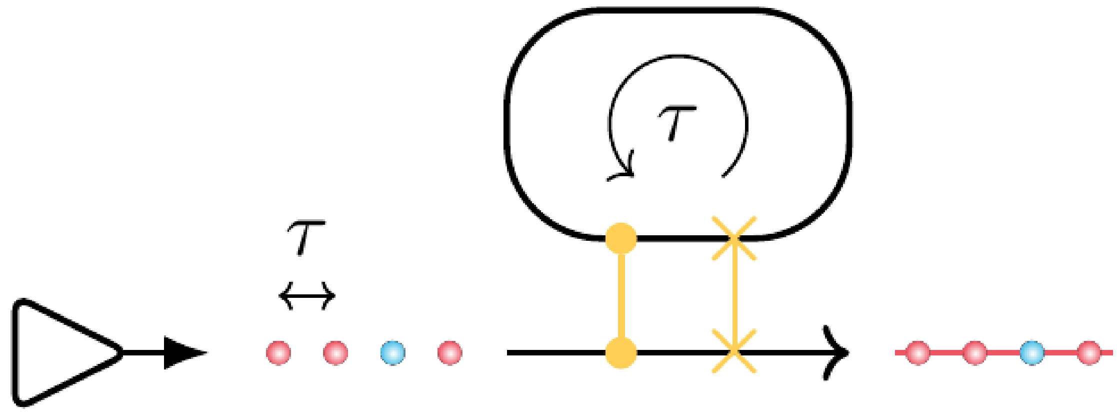

(a)

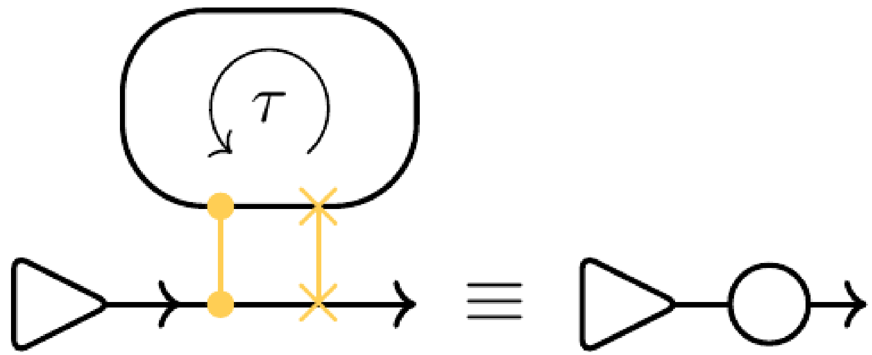

(b)

Figure 4: **Generating 1D qubit cluster in the time domain**. (a) On the left, a 'GBS factory' comprising multiplexed GBS devices is used to generate the sequence of pulses, where each pulse contains either a GKP $|+\rangle$ state or a momentum-squeezed state. Each input interacts with the previous input (which is in the loop) via a CZ gate, enters the loop mode via the swap, interacts with the next mode, and then is swapped into the output mode by the same swap. (b) Simplified diagram for 1D time-domain cluster state source.

Figure 16: A review of optical implementations of the gates and measurements required for Clifford operations in the GKP encoding, including limits required to achieve ideal, perfect CV gate application. (a) A general displacement module [176]. Displacement by $\sqrt{\pi}$ in q (p) corresponds to a GKP qubit Pauli X (Z) gate. (b) Rotation module as performed by e.g. an optical thermoelectric heating element. $\phi = \pi/2$ corresponds to the CV Fourier transform as well as the GKP-qubit Hadamard gate. (c) Homodyne measurement module. Changing the rotation ϕ changes the axis in phase space along which the measurement is performed. $\phi = 0$ ($\pi/2$) corresponds to q (p) homodyne measurement, which is the GKP qubit Pauli Z (X) measurement. (d) Measurement-based squeezing module [168]. On-demand, in-line squeezing is in general required for implementing CV quadratic phase and Controlled-X/phase gates, and a measurement-based approach allows for offline preparation of squeezed resource state. (e) Quadratic phase gate module [177]. $s = \pm 1$ corresponds to the GKP qubit phase gate. (f) CV CZ gate module. $s = \pm 1$ corresponds to the GKP qubit CZ gate. Application of $\pi/2$ rotations on the second mode before and after the CZ gate implements a CV CX gate [177] with Target state 1 becoming the control and Target state 2 becoming the target, and thus a GKP qubit $CNOT$ gate.

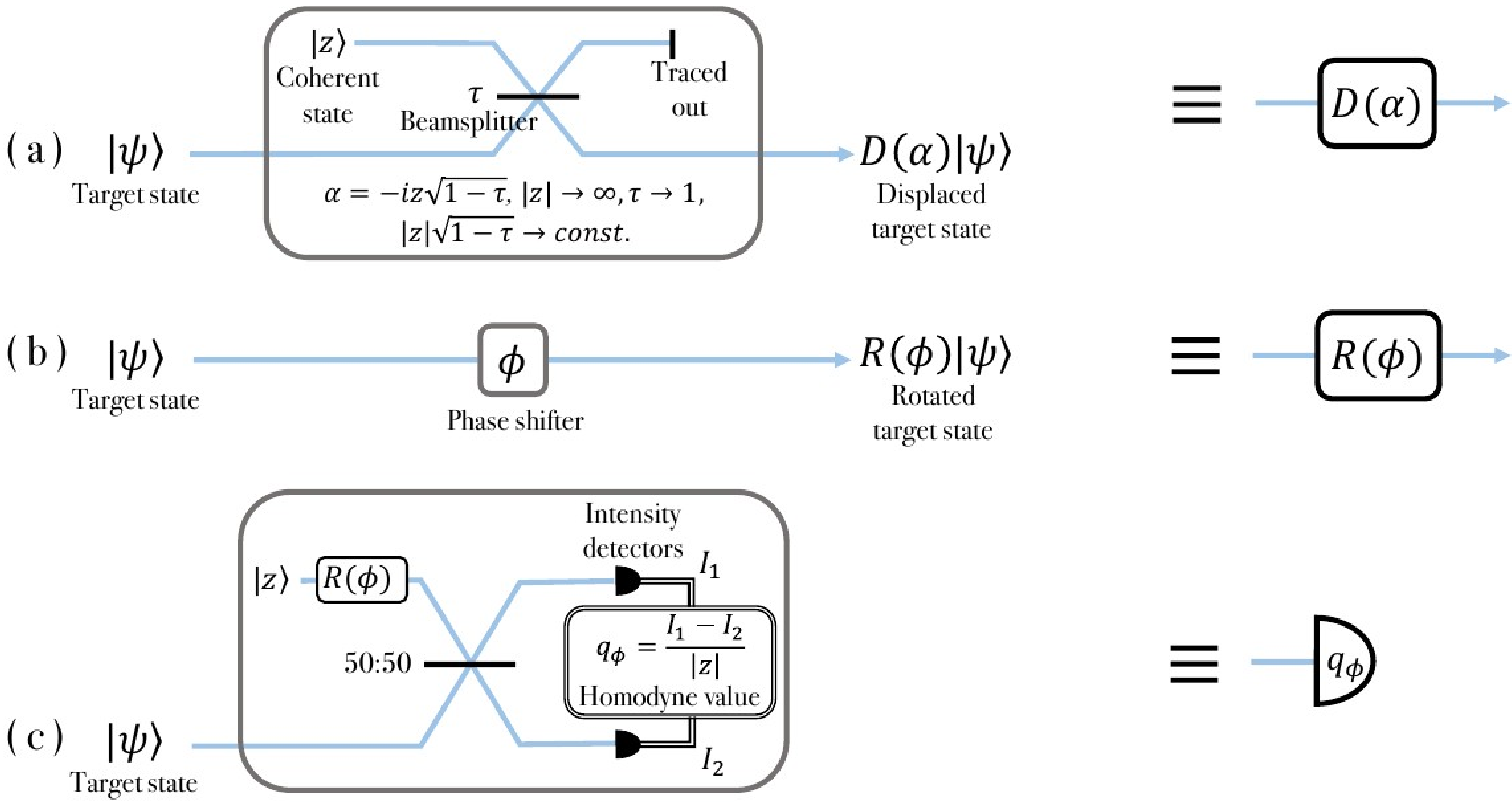

(a)
$|\psi\rangle$
Target state
$|z\rangle$
Coherent state
τ
Beamsplitter
Traced out
$\alpha = -iz\sqrt{1-\tau}$, $|z| \to \infty, \tau \to 1,$
$|z|\sqrt{1-\tau} \to const.$
$D(\alpha)|\psi\rangle$
Displaced target state
$\equiv$
$D(\alpha)$
(b)
$|\psi\rangle$
Target state
ϕ
Phase shifter
$R(\phi)|\psi\rangle$
Rotated target state
$\equiv$
$R(\phi)$
(c)
$|\psi\rangle$
Target state
$|z\rangle$
$R(\phi)$
50:50
Intensity detectors
I_1
I_2
$q_\phi = \frac{I_1 - I_2}{|z|}$
Homodyne value
$\equiv$
q_ϕ

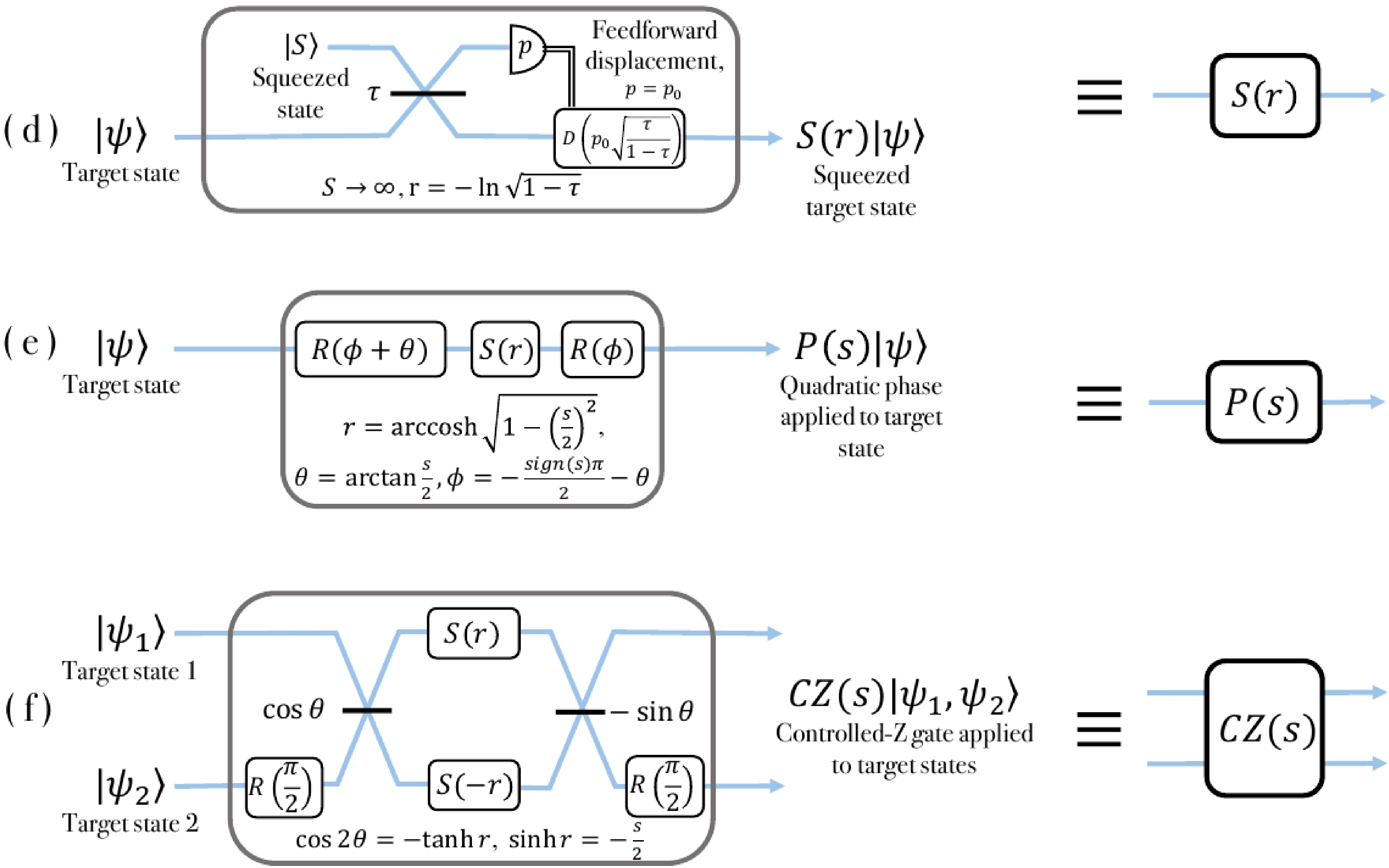
(d)
$|\psi\rangle$
Target state
$|S\rangle$
Squeezed state
τ
p
Feedforward displacement, $p = p_0$
$D\left(p_0\sqrt{\frac{\tau}{1-\tau}}\right)$
$S \to \infty, \mathrm{r} = -\ln\sqrt{1-\tau}$
$S(r)|\psi\rangle$
Squeezed target state
$\equiv$
$S(r)$
(e)
$|\psi\rangle$
Target state
$R(\phi+\theta)$
$S(r)$
$R(\phi)$
$r = \mathrm{arccosh}\sqrt{1-\left(\frac{s}{2}\right)^2},$
$\theta = \arctan\frac{s}{2}, \phi = -\frac{sign(s)\pi}{2} - \theta$
$P(s)|\psi\rangle$
Quadratic phase applied to target state
$\equiv$
$P(s)$
(f)
$|\psi_1\rangle$
Target state 1
$|\psi_2\rangle$
Target state 2
$\cos\theta$
$S(r)$
$S(-r)$
$R\left(\frac{\pi}{2}\right)$
$-\sin\theta$
$R\left(\frac{\pi}{2}\right)$
$\cos 2\theta = -\tanh r,\ \sinh r = -\frac{s}{2}$
$CZ(s)|\psi_1, \psi_2\rangle$
Controlled-Z gate applied to target states
$\equiv$
$CZ(s)$

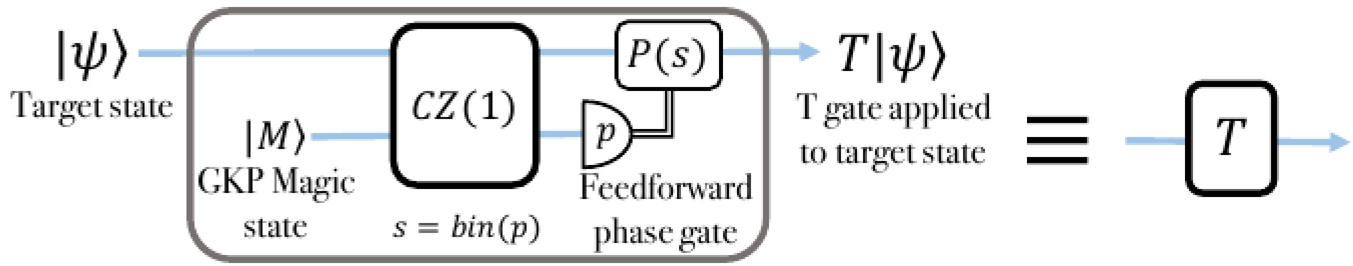

Figure 17: Optical implementation of the GKP qubit T gate up to global phase, following the method from [20]. Here, in the ideal limit, $|M\rangle = e^{-i\pi/8}\,|+\rangle_{\mathrm{gkp}} + e^{i\pi/8}\,|-\rangle_{\mathrm{gkp}}$, and the feedforward phase gate is applied if the ancillary mode detects $|-\rangle_{\mathrm{gkp}}$ via a qubit X measurement (CV p homodyne).

"Half"

Which type of components are needed ?

Deterministic generation

First

Rotating

$$P^{(1)}_{i\to f}(t) = \left|C^{(1)}_f(t)\right|^2 = \frac{|(\hat{\mathbf{d}}\cdot\mathbf{E}_0)_{fi}|^2}{\hbar^2}\,\frac{\sin^2(\Delta t/2)}{\Delta^2}$$

$$\mathcal{G}(|\psi\rangle) \equiv \log_2\left(\sum_{i,j\in\mathbb{F}_2^n}\left|\sum_{k\in\mathbb{F}_2^n}\frac{(-1)^{i\cdot k}}{2^n}c_k\,c^*_{k+j}\right|\right)$$